Fifteen Minutes of *fim*:
Control of Type 1 Pili Expression in *E. coli*

DENISE M. WOLF[1] and ADAM P. ARKIN[1,2]

ABSTRACT

Pili are used by *Escherichia coli* to attach to and invade mammalian tissues during host infection and colonization. Expression of type 1 pili, believed to act as virulence factors in urinary tract infections, is under control of the '*fim*' genetic network. This network is able to sense the environment and actuate phase variation control. It is a prime exemplar of an integrative regulatory system because of its role in mediating a complex infection process, and because it instantiates a number of regulatory motifs, including DNA inversion and stochastic variation. With the help of a mathematical model, we explore the mechanisms and architecture of the *fim* network. We explain (1) basic network operation, including the roles of the recombinase and global regulatory protein concentrations, their DNA binding affinities, and their switching rates in observed phase variation behavior; (2) why there are two recombinases when one would seem to suffice; (3) the source of on-to-off switching specificity of FimE; (4) the role of *fimE* orientational control in switch dynamics; and (5) how temperature tuning of piliation is achieved. In the process, we identify a general regulatory motif that tunes phenotype to an environmental variable, and explain a number of apparent experimental inconsistencies.

INTRODUCTION

TYPE 1 PILI, adhesive organelles expressed on the surface of *Escherichia coli*, are believed to be important in establishing and maintaining infection in a human host. The genetic circuit controlling type 1 pili expression in *E. coli* is an attractive model system not only because of its role in infection, but also because it instantiates a number of more general regulatory motifs. The circuit contains an invertible DNA element, a device found in many other genetic networks (Komano, 1999; Tominaga et al., 1991; van de Putte et al., 1980). Stochasticity, a salient feature of the *fim* control network, was recently identified to be an important source of nongenetic diversity in bacteria (McAdams and Arkin, 1997). Also of general interest is the ability of this circuit to balance a set of competing and conflicting demands for survival within a host environment.

In this paper we analyze the genetic circuit responsible for type 1 piliation control. We identify the architectural features of the network that enable it to sense the environment and control phase variation be-

[1]Lawrence Berkeley National Laboratory, Berkeley, California.
[2]Departments of Bioengineering and Chemistry, University of California at Berkeley, Berkeley, California.

havior in such a way as to balance the conflicting demands of infection and immune system avoidance, and offer explanations for a number of apparent experimental inconsistencies. In addition, we find a number of interconnected regulatory motifs, subnetworks whose general architecture and operating principles are found in other biological systems, which are interconnected to achieve the overall function of the circuit.

Background

Urinary tract infections (UTI) form the context for type 1 piliation control. These infections, including cystitis and pyelonephritis, affect over seven million people annually in the United States alone. Uropathic *E. coli* (UPEC) are thought to be responsible for 70–95% of UTIs, of which 25% are persistent and recurrent (Barnett and Stephens, 1997; Hooton and Stamm, 1997).

During the course of an infection, *E. coli* encounter a plethora of host defenses. Active defenses include flushing, via micturition, exfoliation of infected and adherent host cells, influx of neutrophils into the urothelium and bladder, and second and third wave immune responses (Mulvey et al., 2000). UPEC strains contain a number of virulence factors enabling infection despite these defense mechanisms. Foremost among these virulence factors are type 1 pili, the subject of our analysis (Connell et al., 1996; Langermann et al., 1997; Schaeffer, 1987).

Type 1 pili are capable of mediating attachment to the mannose-containing receptors found in many host tissues. The pili consist of 7-nm-thick helical rods made up of repeating FimA subunits connected to a 3-nm-wide tip containing two adapter proteins, FimF and FimG, and the adhesin, FimH (Jones et al., 1995; Russell and Orndorff, 1992). Interactions between FimH and luminal surface receptors on the bladder epithilium enable UPEC strains to colonize the bladder and cause disease (Langermann et al., 1997; Martinez et al., 2000; Sauer et al., 2000).

Type 1 pili are thought to aid the infection and colonization process by two mechanisms: adherence and invasion. Without a means of adhering to host tissues, micturition would extinguish all but the fastest growing strains (Gordon and Riley, 1992). The adhesin FimH mediates invasion by activating a phagocytic process in host cells (Sauer et al., 2000). Once inside the host cells, *E. coli* either replicate and flux from the cell or become quiescent. Internalization provides opportunies for rapid replication and a means to avoid the immune system (Martinez et al., 2000).

While pili provide a means for infection, they also activate an inflammatory response. This activation can rapidly clear infection through enhanced neutrophil and other immune cell recruitment and massive exfoliation (Bergan, 1997). Hence, there is a trade-off between the virulence conferred by type 1 pili and the host immune response to a piliated bacterial population. The genetic network controlling piliation is thought to balance this trade-off.

Figure 1 diagrams the genetic circuit controlling the expression of type 1 pili. The core of this circuit is a 314-bp length of invertible DNA known as the '*fim* switch' (Abraham et al., 1985). This invertible element contains the promoter for the *fim* structural subunit genes (*fimA-fimH*). The promoter directs transcription only when the switch is in the on position (Gally et al., 1993; Klemm, 1986; McClain et al., 1991). Because the switch flips back and forth due to action of the recombinases and global regulators, individual cells can alternate between densely pilated and unpilated states, a process known as phase variation. Phase variation yields a heterogenous population of piliated and unpiliated cells. The population of piliated cells is controlled by the environment (Gally et al., 1993), the phase of infection, and the host immune response (Bergan, 1997). Evidence indicates that the *fim* network senses the environment and creates a population with enough piliated cells to establish infection and create quiescent pockets for recurrence, but not so many as to trigger a coordinated immune response (M. Mulvey, personal communication; Schilling et al., 2001).

Questions addressed

Though much is known about the molecular details of the *fim* genetic circuit (Fig. 1), system level questions remain. Most basic of these is how the circuit senses the environment and controls the piliation level, bacterial attachment, detachment, and invasion rates of the population. This question, in turn, leads to ques-
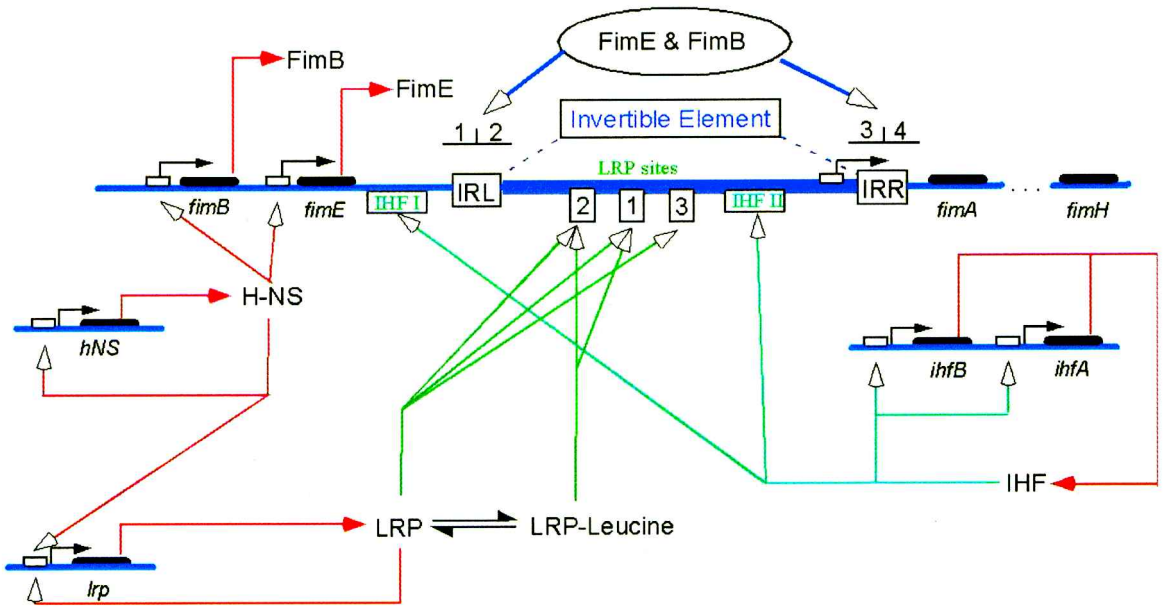
FIG. 1. Genetic network controlling type 1 pili phase variation in *E. coli*. Recombinases FimE and FimB act independently to invert the invertible DNA element (Gally et al., 1993; Klemm, 1986; McClain et al., 1991) and have been shown to bind to four half-sites flanking the switch boundaries (Gally et al., 1996). FimE biases the recombination in the on-to-off direction ($\approx.3$/cell/generation) (Gally et al., 1993; Klemm, 1986; McClain et al., 1991), while FimB is relatively unbiased ($\approx 10^{-4}$/cell/gen; Gally et al., 1993). The expression of *fimE* is orientationally controlled, meaning that it is expressed when the *fim* switch is in the on position, but is not detectably expressed when the switch is off (Kulasekara and Blomfield, 1999). In addition to FimB and FimE, global regulating proteins IHF, Lrp, and H-NS play a supporting role in *fim* switch control. IHF, necessary for any observable switching to occur, is believed to help 'bend' DNA into a loop (Blomfield et al., 1997). Lrp dimers bind to three sites within the switch and increase switching rates in both directions. This effect is amplified by the presence of leucine (Roesch and Blomfield, 1998). Protein H-NS represses transcription of *fimE*, *fimB*, and *lrp* in a temperature-dependent manner (Olsen and Klemm, 1994; Olsen et al., 1998; Oshima et al., 1995). In addition, local transcription from within *fimE* toward the switch, in conjunction with H-NS activity, contributes to the observed on-to-off switching bias of *fim* (O'Gara and Dorman, 2000). Genes *lrp*, *ihfA*, *ihfB* and *hNS* are all known to be self-regulating via repressive binding to their own promoters (Bykowski and Sirko, 1998; Ueguchi et al., 1993; Wang et al., 1994).

tions about the design of the circuit. For example, why does the network have two recombinases, when other invertible systems have just one? Are the recombinases redundant, or does the two-recombinase design confer some special property to the system? Given that the two recombinases have similar sequences and bind to nearly identical sites along the switch, why is FimE switching strongly biased towards the off direction when FimB switching is relatively unbiased (Kulasekara and Blomfield, 1999)? What role does *fimE* orientational control—the phenomenon where FimE is only expressed when the switch is in the on position—play in the function of the circuit (Kulasekara and Blomfield, 1999)? How does *E. coli* sense it is in the host? And how does the *fim* network architecture determine that the environment is at 37°C and respond by increasing switching rates and the piliation level of the population (Gally et al., 1993; Roesch and Blomfield, 1998)?

We address these questions using a synthetic analysis of whole network function. Such an analysis requires that we construct a mathematical model of the *fim* circuit. Using this model, we propose answers to the above questions and show how interactions between the recombinases, regulatory proteins, and the switch DNA mediate phase variation control.

MATHEMATICAL MODEL ASSUMPTIONS

The model consists of differential equations, described in Appendix A. The model is based on the following data and assumptions:

- We assume the 314-bp invertible element is binary, that is, either on or off. We base this assumption on data implying that any intermediate configurations or complexes, if they exist, are short lived relative to the flipping rate of the switch (Abraham et al., 1985).
- We assume that inversion is governed by a stochastic process mediated by cellular proteins. This assumption yields the master equation form of Equations 1 and 2 in Appendix A. Slow flipping rates and the fact that each cell contains a single copy of the *fim* switch preclude use of an averaged, deterministic model.
- The regulatory proteins directly included in our model are the recombinases FimE and FimB and the global regulators IHF and Lrp. These proteins have been found to bind directly to the switch DNA and mediate inversion rates (Blomfield et al., 1997; Gally et al., 1993; Klemm, 1986; McClain et al., 1991; Roesch and Blomfield, 1998). The action of H-NS is modeled indirectly, through its temperature- and nutrient-mediated repression of the recombinases and Lrp (Donato et al., 1997; Olsen and Klemm, 1994; Olsen et al., 1998; Oshima et al., 1995).
- Regulatory proteins FimB, FimE, IHF and Lrp are assumed to be in quasi-equilibrium with the switch DNA. This assumption yields a Shea-Ackers (Shea and Ackers, 1985) form for switch inversion rates *f* and *g* in Equations 1 and 2 (Appendix A).
- We simplified the four FimE/FimB half-sites flanking (in pairs) the boundaries of the switch (Gally et al., 1996) into a single binding site $P_{FimE/B}$. Given the lack of information on the number of molecules that bind (1, 2, or 4), we chose the simplest configuration. Our purpose was to encode (a) competitive binding between FimE and FimB, (b) the necessity of one of the two species binding for switching to occur, and (c) the dependence of switching rates in both directions on the recombinases and global regulators. A consequence of this abstraction is the elimination of one source of cooperativity in switching behavior and the exclusion of a number of inactive molecular states. Computer experiments with additional FimE/B binding sites included in the model demonstrated that this simplification would not alter our results.
- We simplified Lrp binding sites 1 and 2 into the single (two-dimer) site Lrp-A. We made this simplification because the two sites are highly cooperative (Roesch and Blomfield, 1998).
- Our model includes Lrp binding site 3 (Lrp-3) as a separate site. This site is known to have a lower binding affinity than the others, and plays a functional role in switching rate control (Roesch and Blomfield, 1998).
- The two IHF binding sites are simplified into a single site P_{IHF}. This simplification was made because of a lack of information on differential binding/functionality of the two sites, along with our intent to encode the experimental finding that IHF is required for any switching to occur (Blomfield et al., 1997).
- In our model, regulatory proteins FimE, FimB, IHF, and Lrp interact with the switch DNA by binding and unbinding to their respective binding sites $P_{fimE/B}$, P_{IHF}, Lrp-A, and Lrp-3, and, once bound, by mediating inversion. There are 36 different molecular configurations possible, as listed in Table 1. Each molecular configuration in Table 1 yields a different switching rate. Switching, a function of the occupancy of regulatory binding sites, can occur only when IHF and either FimE and FimB are bound to the invertible element.
- We model the orientational control of *fimE*. FimE is expressed only when the switch is in the on position (Kulasekara and Blomfield, 1999). However, we do not model H-NS sensitive local transcription from within *fimE*, an additional source of on-to-off switching bias largely subsumed by the recombinase switching rates in our model (O'Gara et al., 2000).[1]

---

[1]Local transcription from within *fimE* creates a switching bias in the off direction in a mutant with a nonfunctional *fimE* (containing the intact intra-gene promoter sequence). Our model does not capture this mutant.

- We assume environmental control of phase variation is achieved directly through changes in intracellular temperature and amino acid concentrations, and indirectly through changes in the intracellular concentrations of the recombinases and global regulators (Donato et al., 1997; Gally et al., 1993; Landgraf et al., 1996; Olsen and Klemm, 1994; Olsen et al., 1998; Oshima et al., 1995; Roesch and Blomfield, 1998). Different concentrations of intracellular proteins lead to different probabilities of molecular occupancy of the switch binding sites. Since each molecular configuration in Table 1 is associated with a different switching rate, different environmental conditions lead to different switching rates, and thus to different piliation levels, response times, attachment rates and detachment rates of the *E. coli* population.

Appendix A provides a detailed description of the model and its derivation. System parameters include FimE and FimB mediated switching rates α_i, with and without Lrp bound to the switch, and the Gibbs free energy ΔG_i of each possible molecular configuration (Tables 1, 3, and 4). As described in Appendix C, some of these parameters have been experimentally determined, though most were estimated. Because our analysis relies primarily on symbolic computation rather than numerical simulation, the results in this paper are largely independent of the parameters; however, we have included them for the sake of completeness and to help the interested reader set up a simulation.

MODEL RESULTS

In this section, we briefly describe how the circuit operates and answer the design questions posed in the introduction. These questions are largely separable, and we answer them one by one. At the end of the paper we present an integrated view of how phase variation control is achieved through the combination of these control modules.

Phase variation control

Population level control variables: Piliation level and response time. Phase variation behavior is characterized by two variables, P^*_{on} and τ (see Figure 2 and Appendix B). P^*_{on} is the mean fraction of the population with switches in the on position—and thus presumably piliated—at steady state. τ is the response speed of the switch, specifically the amount of time it takes $P_{on}(t)$ to reach 63.2% (1/e) of its steady state value P^*_{on} starting from an initial condition of $P_{on}(0) = 0$. In disease process terms, P^*_{on} is proportional to the rate at which bacteria attach to the urothelium, and τ is the amount of time it takes a population to move from one steady-state %ON to another in response to the environment, for example, a fever induced by immune response to infection.

The fim network is a recombinase ratio controlled switch. By analyzing how P^*_{on} and τ depend on recombinase and global regulator concentrations and on the physical parameters in our model, which consist
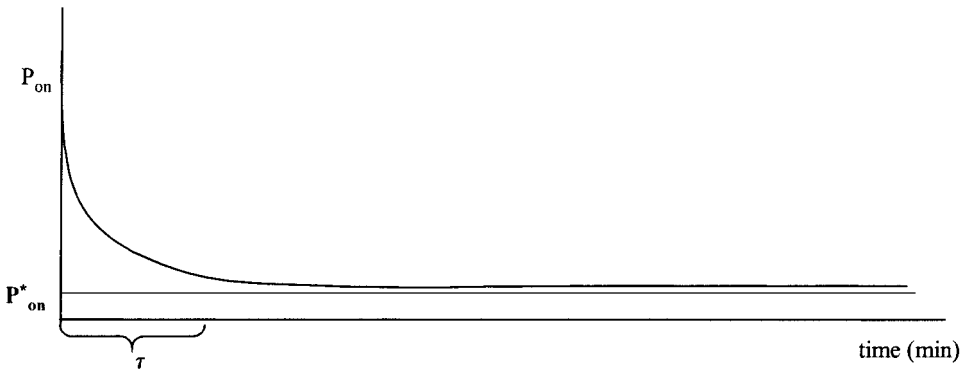

FIG. 2. Single stable stationary phase of the *fim* switch. The mean population-fraction with switches in the on position, P_{on}, follows a trajectory $P_{on}(t)$ characterized by the steady state P^*_{on} and τ, the mean amount of time it takes to reach steady state.

primarily of binding affinities and switching rates associated with different configurations of regulatory molecules bound to the switch DNA (see Appendix B), we found that (a) steady state piliation level P^*_{on} is a sigmoidal, switch-like function of the recombinase ratio [FimE]/[FimB], with asymptotes and slopes depending on physical parameter ratios and differences, (b) response time τ is sigmoidally controlled by the recombinase ratio as well, but also is quite sensitive to absolute recombinase concentrations and the absolute values of physical parameters, and (c) there is a decoupling between the control of steady state piliation level and response time. The biological relevance of these findings is discussed later in the paper.

Figure 3 illustrates these results, and Table 2 provides the details of how the asymptote heights and transition region slopes depend upon the physical parameters. Intuitively, one can understand recombinase ratio control as follows. Consider the action of the two recombinases on the invertible element in isolation and assume that FimE and FimB bind to the switch with the same affinity. The mean steady state piliation level is determined by the relative frequency of on-to-off and off-to-on switching. Both FimE and FimB contribute to these switching rates (see Appendix A). If [FimB] $>>$ [FimE], then FimB-mediated switching rates dominate and the population will be equally divided between piliated and unpiliated cells once it reaches steady state (left side of sigmoid in Fig. 3). If [FimE] $>>$ [FimB], then FimE-mediated (off-biased) switching rates dominate and the population will be largely unpiliated (right side of sigmoid in Fig. 3). Though each individual switching rate depends on the absolute value of a recombinase concentration (assuming unsaturated binding sites), P^*_{on} depends only on the recombinase ratio [FimE]/[FimB] and *not* on the absolute concentrations of the individual recombinases. Increasing or decreasing [FimB] and [FimE], while keeping their ratio constant, will have no effect on the piliation level of the population (or on attachment rates to the urothelium).

The same cannot be said for the response time. The amount of time the system takes to reach steady state depends upon the absolute concentrations of the recombinases as well as the recombinase ratio. Even at a fixed recombinase concentration ratio, more recombinase means more frequent switching, and thus faster convergence to steady state. This simple example also illustrates an aspect of the decoupling of piliation level and response time control. Response time and detachment rate can be varied without changing piliation level or attachment rate. Any change in environment or growth phase affecting the expression of both recombinases equally (and thus maintaining a constant recombinase ratio) will have this effect. There is an asymmetry in this decoupling of control, however, as changing piliation level and attachment rate, without a concurrent change in response time and detachment rate, is not possible.

Naturally, the whole *fim* model, complete with variable binding affinities, global regulators and *fimE* orientational control, is not so simple. These additional factors play a role in control through their influence on the heights of the control sigmoid asymptotes and the steepness of the transition region slopes, and through their affect on $p_{on\text{-}off}(t')$, the probability distribution of the time it takes a switch to turn off (see Figs. 3 and 6 and 7 below, and Table 2). For example, binding affinity differences between FimB and FimE determine the sharpness of the slopes of the sigmoid transition regions, and thus the effective Hill coefficients of the control curves. At high recombinase concentrations, switching rate ratios and differences in cooperativity between IHF and each recombinase in the two switch positions influence sigmoid asymptote heights. At very low recombinase concentrations, with the switch binding site $P_{fimE/B}$ relatively unoccupied, sigmoid asymptotes are affected by differences in the binding affinities of each recombinase in the on and off switch positions. Lrp concentration influences phase variation control in large part by determining which switching rates and binding affinities dominate the sigmoid parameters described above. The free energies of binding of each recombinase to the switch DNA, and the switching rates of each recombinase, depend upon the occupancy of Lrp binding sites, and thus on the concentration of Lrp (see Table 1). This effect is manifested in non-monotonic control surfaces like the one shown in Figure 4 and produces the temperature tuning discussed later in the paper. Despite these complexities, the basic themes of phase variation control as described above hold true in the complete model.

Effect of two recombinases

Having described some basic features of phase variation control, we address the question of whether the fundamental properties of piliation control in the two-recombinase design (i.e., sigmoidal, switch-like recombinase ratio control and decoupling of the control of piliation level and attachment rate and response
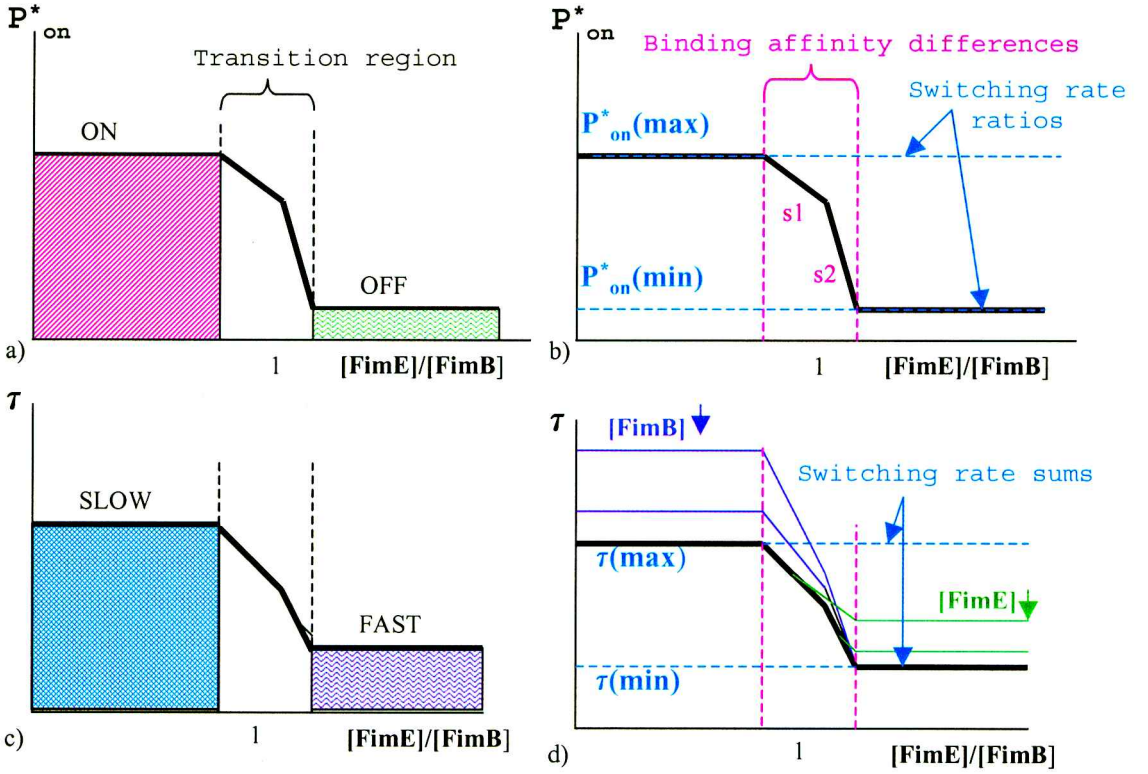
FIG. 3. Dependence of P^*_{on} and τ on the recombinase ratio [FimE]/[FimB]. (**a**) P^*_{on}, the steady state fraction of pili-ated bacteria, is a sigmoidal, switch-like function of the recombinase ratio [FimE]/[FimB], which determines whether the population is strongly off ([FimE]>>[FimB]), weakly on ([FimB]>>[FimE]), or in transition ([FimB] ≈ [FimE]). (**b**) The piliation control sigmoid is defined by its asymptotes P^*_{on} (max) and P^*_{on}(min) and transition region slopes s1 and s2. The former are functions of switching rate ratios and the latter of binding affinity differences (Table 2). (**c,d**) The re-sponse time of the system, τ, is also a sigmoidal function of [FimE]/[FimB], but is sensitive to the absolute values of the recombinases and system parameters in addition to the ratios and differences dominating P^*_{on} (Table 2). When [FimE] >> [FimB], the response is much faster ($\tau = \tau_{min}$) than it is when [FimB] >> [FimE] ($\tau = \tau_{max}$). Consequently, switch-ing from a weakly on to a strongly off population occurs much more rapidly than does a switch in the other direction.

time and detachment rate) would also be present in a single recombinase version of the system. To inves-tigate, we simulated a *fimE*[-] mutant and analyzed P^*_{on} and τ for their dependencies on the recombinases, global regulators, and system parameters. We found the following differences between single and double recombinase action.

Two recombinases are necessary for sigmoidal, switch-like behavior. With a single recombinase, the switch-like character of the control is greatly diminished (Fig. 5). In our simple example of identical bind-ing affinities for the switch DNA in the off or on positions, not only is piliation level P^*_{on} not a sharp sig-moidal function of recombinase concentration, it is a constant. In the complete system, the main source of a differential in steady state piliation levels at very high and very low recombinase concentrations are bind-ing affinity and cooperativity differences. Specifically, differences in the amount of cooperativity between the recombinase and IHF, when the switch is in the on position or in the off position, affect the steady-state piliation level at very high recombinase concentrations. At very low recombinase concentrations, differ-ences between the affinity of the recombinase for switch DNA in the on or off positions have an effect on steady-state piliation level. These dependencies, sources of minor variation between piliation and attach-ment levels at different intracellular recombinase concentrations (which do not approach the switch-like character of piliation control with two recombinases in action), are illustrated in Figure 5.
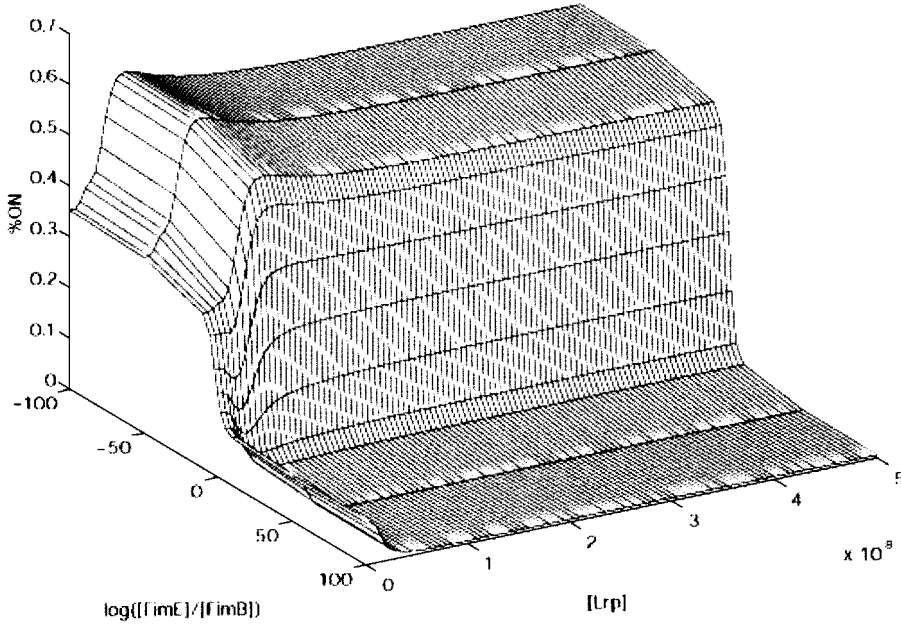
FIG. 4. Fraction of piliated cells as a function of recombinase ratio and Lrp concentration. This function is sigmoidal along the [FimE]/[FimB] axis and inverted-parabolic along the [Lrp] axis at low recombinase ratios.

Single recombinase results in loss of environmental control over piliation level and attachment rate. We assume that environmental control is achieved largely through modulation of the intracellular concentrations of the recombinases and global regulators. For example, recombinase concentrations are known to be sensitive to temperature and medium richness (Free and Dorman, 1995; Olsen et al., 1998). Since removing a recombinase effectively flattens out the curve relating piliation level (and attachment rate) to recombinase concentration, we conclude that a single recombinase system is less sensitive to environmental changes than is the double recombinase design with its sigmoidal control curves.

Decoupling and robustness of control are reduced in a single recombinase system. With a single recombinase, absolute concentrations and parameter values are responsible for all aspects of control. This means that the control of piliation level and attachment rate is coupled to the response time and detachment rate control. Independent control of these behaviors, possible in the two-recombinase design (and perhaps useful for rapid detachment from host cells defended by immune cells), is not an option. Also evident is a
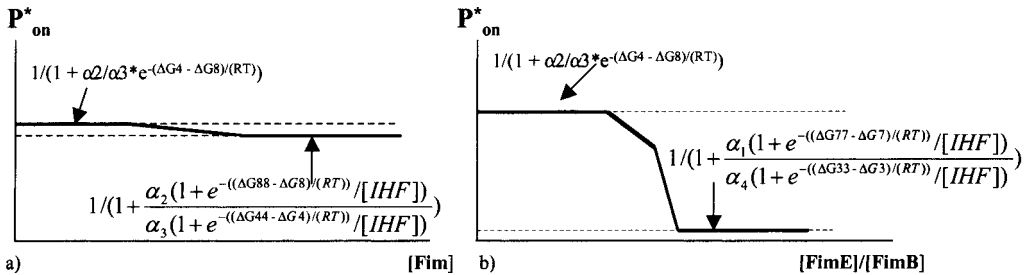

FIG. 5. Comparison of P^*_{on} in single and double recombinase models. (**a**) With a single recombinase, the *fim* genetic circuit cannot act as a small-signal switch. The high and low asymptotes of P^*_{on} are nearly equal because they are both dominated by the same switching rate ratio α_2/α_3. (**b**) With two recombinases P^*_{on} is a sigmoidal function of recombinase ratio, with the high asymptote dominated by α_2/α_3 and the low asymptote dominated by α_1/α_4 ($\alpha_1/\alpha_4 \ll \alpha_2/\alpha_3$).

difference in robustness between one- and two-recombinase systems. Since piliation level in the two-recombinase system is independent of absolute concentrations and reaction rates, it is robust to drift, an engineering term for uniform shifts in protein concentrations or reaction rates due to genetic variation and environmental factors. The single recombinase system is sensitive to these shifts, in contrast to the double recombinase design. Robustness is believed to confer a survival advantage to the organism (Alon et al., 1999; Barkai and Leibler, 1997).

Impact of orientational control on phase variation

Experimental evidence from (Kulasekara and Blomfield, 1999) shows that FimE is significantly expressed when the piliation switch is in the on position, and nearly undetectable when the switch is in the off position, supporting the earlier hypothesis in (Pallesen et al., 1989) that *fimE* is under switch orientational control (OC). We model *fimE* OC with a Markov chain that couples FimE concentration to switch position (Equation 2 in Appendix A). We can use this model to test for the role of *fimE* OC in network operation. An analysis that compares the behavior of the *fim* network with *fimE* OC (Equation 2) to that without it (Equation 1) predicts the following.

Orientational control provides a source of memory for switch position. Without OC, the *fim* network is a memoryless system with no way of knowing how long the invertible element has been in the on or off state. The OC of *fimE* provides the network with a source of feedback and memory. When the switch is off, [FimE] is close to zero. Upon inversion of the switch, *fimE* expression is turned on. With time, FimE accumulates in the cell. Thus the concentration of FimE holds the memory of the length of time the switch has been in the on position.

Orientational control keeps the switch on long enough to build pili. Figure 6 shows the effect of OC on the on-to-off switching time probability distribution $p_{on-off}(t')$, defined in Appendix B. Without OC this dis-

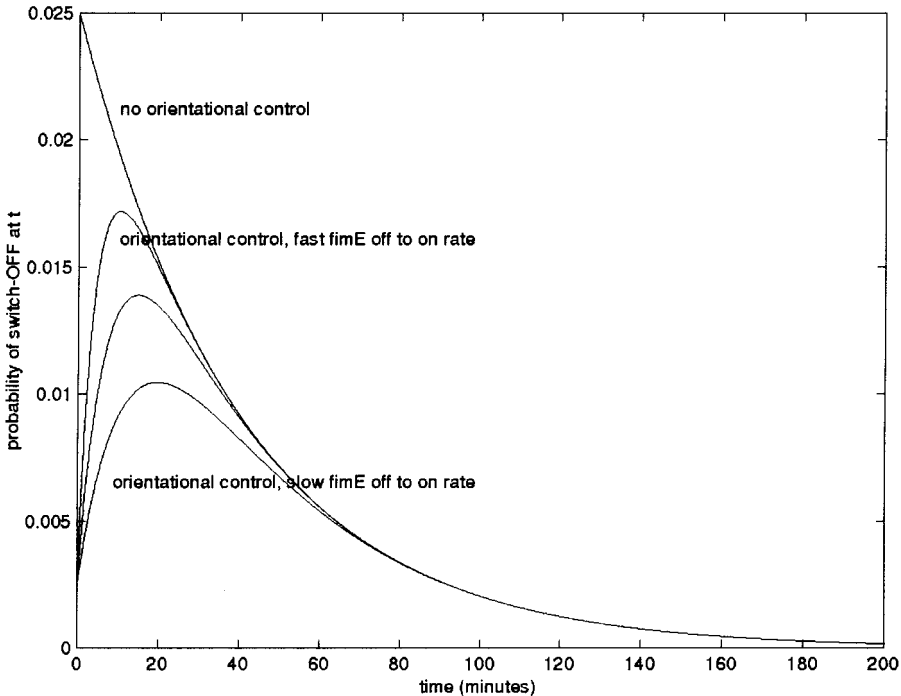**FIG. 6.** Effect of *fimE* orientational control on the on-to-off probability distribution $p_{on-off}(t')$ (the probability that the switch will turn off at time t = t' given that it was turned on at time $t = 0$).

tribution is exponential, while with OC the distribution resembles a log normal. OC has the effect of skewing the amount of time the switch remains on away from zero. As pili construction takes time, OC appears to serve the function of remembering how long the switch has been in the on position, and uses this memory to keep the switch on long enough to densely coat the cell with pili. This feature is likely important in environmental conditions with low [FimB], such as in rich medium at low temperature. Without the competitive inhibitory effect of FimB, FimE mediated on-to-off switching is exceedingly rapid (Gally et al., 1993; Roesch and Blomfield, 1998).

Orientational control increases sensitivity of P^*_{on} to [FimB] and the environment. Without OC, the fraction of piliated cells at steady state is a robust and highly cooperative function of the recombinase ratio [FimE]/[FimB]. As shown in Figure 7, while P^*_{on} with OC in operation is still a sigmoidal function of the recombinase ratio, it depends also on the absolute amount of [FimB] present in the cell. Since we assume that environmental control is achieved largely through mediation of recombinase concentrations, we conclude that this dependence results in an increased sensitivity of P^*_{on}, and thus attachment and invasion rates, to changes in environmental conditions like temperature and medium. This increased sensitivity is achieved by amplifying the effect of differential de-repression of the two recombinases by temperature- and medium-controlled H-NS (Donato et al., 1997; Olsen and Klemm, 1994; Olsen et al., 1998). An increase in temperature leads to a decrease in H-NS concentration and/or activity, which leads to differential de-repression of *fimB* and *fimE*. This de-repression results not only in a decrease in recombinase ratio (and accompanying slide across the piliation control sigmoids), but also in an increase in [FimB] (and increase in asymptotes). Together, these shifts lead to a greater increase in piliation and attachment rates than would be possible without *fimE* OC.

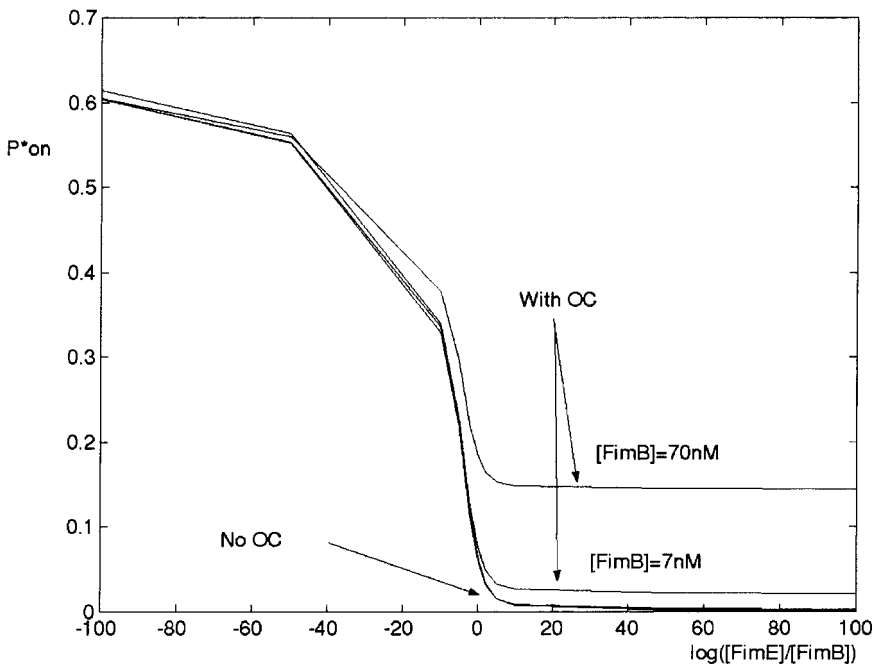**FIG. 7.** Sensitivity of piliation to [FimB] and to the recombinase ratio [FimE]/[FimB] with *fimE* orientational control (OC). Since environmental control of the network is accomplished in part through differential de-repression of *fimB* and *fimE* by H-NS, this added sensitivity to [FimB] translates into an increase in environmental responsiveness of the network.

Sources of FimE on-to-off specificity

Considering that FimE is homologous to FimB and that the two recombinases bind to overlapping, nearly identical sites (Gally et al., 1996), the source of strong on-to-off switching preference of FimE, as compared to the relatively unbiased FimB switching, has been a mystery. It was hypothesized that differences in DNA binding affinities of FimE and FimB account for this specificity, though Leathart and Gally (1999—white paper) and (Kulasekara and Blomfield, 1999) found these differences insufficient and (Kulasekara and Blomfield, 1999) hypothesized a complementary role for the orientational control of *fimE*.

Our model suggests that FimE's switching specificity is due primarily to switching rate ratios rather than binding affinity differences between FimE and FimB, and predicts a paradoxical role for *fimE* orientational control.

System conditions determine whether binding affinities or switching rates are responsible for FimE specificity. DNA binding affinity differences between FimB and FimE determine the degree of cooperativity, and thus the sensitivity of the system, to small perturbations of the recombinase ratio away from the inflection point (Fig. 3 and Table 2). Yet $P^*_{on}(min)$, the minimum piliation level of a population, is predominantly a function of the ratio between the FimE mediated on-to-off and off-to-on switching rates (α_1/α_4) and *not* a function of DNA binding affinities. Thus, the source of FimE specificity depends upon the operating points of the system. If the intracellular values of the recombinases fall within the narrow, sloped transition zone surrounding the inflection point of the sigmoid, then differences in DNA binding affinity play an important role in determining FimE specificity. If, in contrast, the system operates outside of this transition zone, moving from one asymptote to the other as the population changes its composition from weakly-on to strongly-off and vice versa, then differences in switching rates are responsible for the observed FimE specificity.

Experimental determination of the recombinase ratios at different steady-state piliation levels is needed in order to distinguish between these two possibilities. Results showing point mutations in FimE that do not affect binding affinity, but greatly reduce switching bias (Stentebjerg-Olesen et al., 2000), support the idea that binding affinities are not the dominant factor.

How fimE *orientational control affects FimE specificity.* Our model predicts that *fimE* OC lessens FimE specificity in that the time a switch spends in the on position, and the fraction of piliated cells in a population, is greater with OC (Fig. 7). If a mutant FimE happened to have a high off-to-on switching rate, however, and if FimE were extremely unstable, *fimE* OC would maintain the specificity of FimE. In this sense, OC acts as a redundant mechanism to the switching rate ratio induced specificity described above. In fact, our model predicts that FimE switching specificity and *fimE* OC together prevent the system from chattering, or rapidly alternating between on and off states. Chatter would undermine the utility of the *fim* network, a hard switch executing a concrete, binary decision. When the switch is in the off state, the two mechanisms, rate-ratio based specificity and OC, are mutually reinforcing.

Temperature tuning mechanism

Temperature tuning of bacterial gene expression is believed to be an important component of bacterial pathogenicity. Experiments described in (Gally et al., 1993) show that at 37°C piliation is 10-fold higher than at 28°C. Switching from on to off (both FimB and FimE present) was observed to occur faster at lower temperatures in rich nutrient media, while FimB-promoted (only FimB present) switching from off to on increases with temperature, with a maximum switching rate near 37°C (Gally et al., 1993).

Gally et al. (1993), Olsen and Klemm (1994), and Olsen et al. (1998) speculated that it is the H-NS modulation of the expression of type 1 fimbriae that is responsible for a favored fimbriate state at mammalian body temperature, though no specific mechanism was proposed. We propose a mechanism whereby H-NS accomplishes this temperature control via monotonic temperature modulated de-repression of *lrp* and accompanying changes in the occupancy of the Lrp binding sites along the switch DNA.

Temperature tuned to mammalian body temperature: an Lrp-mediated mechanism. At low levels, Lrp increases switching, while at high levels, Lrp represses switching. When [Lrp] = 0, the only switching that occurs in a *fimB⁺ fimE⁻* mutant is baseline FimB-mediated switching (Gally et al., 1993). As the concentration of [Lrp] increases, the probability of Lrp being bound to binding site Lrp-A also increases. This increased probability leads to a corresponding increase in the switching rate; the switching rate with Lrp bound to Lrp-A is much greater than that with no Lrp present (Gally et al., 1993; Oshima et al., 1995; Roesch and Blomfield, 1998). As [Lrp] continues to rise, the binding site Lrp-A saturates, and binding site Lrp-3 becomes increasingly occupied (Roesch and Blomfield, 1998). However, having Lrp bound to Lrp-3 in addition to Lrp-A decreases switching rate (Roesch and Blomfield, 1998). As shown in Figure 8, the maximum in the occupancy of site Lrp-A occurs at physiologic concentrations of Lrp at 37°C, which rises monotonically with temperature because of the de-repressing effect of H-NS on Lrp (Oshima et al., 1995). This mechanism creates a maximum in switching frequency and piliation level at mammalian body temperature.

Temperature tuning as an example of a common regulatory motif. This temperature-tuning mechanism is a common regulatory motif (Fig. 9). Other examples include osmoregulatory porin regulation and Beta-Galactosidase operon control. A osmolarity-controlled local maximum in OmpF expression appears to be associated with the binding of phosphorylated OmpR to three sites with varying binding affinities and expression activation/repression potentials (Lan and Igo, 1998; Russo and Silhavy, 1991). Similarly, Beta-Galactosidase activity exhibits a local maximum at the level of Lrp found in wild-type strains (Borst et al., 1996). The *gltBDF* control region, with its multiple Lrp binding sites, appears to be another special case of this general control motif.

Switching rate dependence on temperature: effect of leucine. Consistent with experimental observations (Gally et al., 1993; Roesch and Blomfield, 1998), our model predicts that leucine shifts the maximum in piliation switching rate to a higher temperature. In Roesch and Blomfield (1998), it was reported that a Lrp-
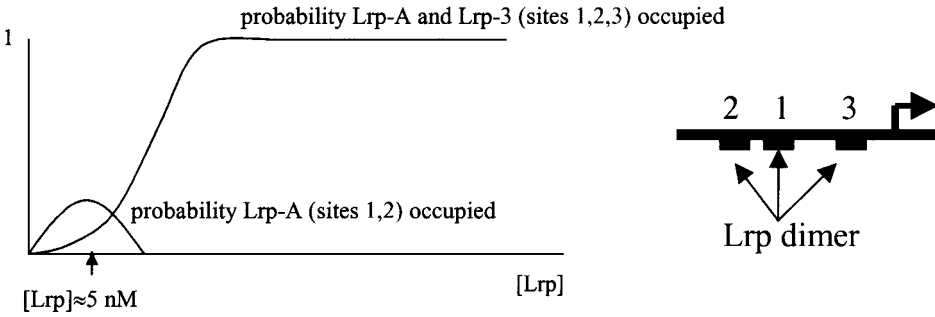

FIG. 8. Site binding probability of Lrp. In modeling the interaction of Lrp with the invertible element, we assume that Lrp is either unbound, bound exclusively to binding site Lrp-A (Lrp bound to sites 1 and 2 in Fig. 1) or bound to both Lrp-A and Lrp-3 (Lrp bound to sites 1, 2, and 3 in Fig. 1). Expressions for the probability that Lrp is bound to Lrp-A only or to both Lrp-A and Lrp-3 are as follows.:

$$p_{Lrp-A} = \frac{e^{-\Delta G_{Lrp-A}/RT}[Lrp]^2}{1 + e^{-\Delta G_{Lrp-A}/RT}[Lrp]^2 + e^{-\Delta G_{Lrp-A,3}/RT}[Lrp]^3},$$

$$p_{Lrp-A,3} = \frac{e^{-\Delta G_{Lrp-A,3}/RT}[Lrp]^3}{1 + e^{-\Delta G_{Lrp-A}/RT}[Lrp]^2 + e^{-\Delta G_{Lrp-A,3}/RT}[Lrp]^3}.$$

As shown in the figure, the probability of Lrp dimers being bound to sites Lrp-1 and Lrp-2 (Lrp-A), but not Lrp-3, first increases and then decreases with an increase in Lrp concentration. Thus there is a local maximum in Lrp-1,2 (Lrp-A) occupancy at some value of Lrp concentration. Using data from (Roesch and Blomfield, 1998) to calculate the free energies (ΔG_{Lrp-A}; $\Delta G_{Lrp-A,3}$) ≈ (−24 kcal; −36.3 kcal) (see Appendix C) and substituting these energies into the above probability expressions revealed the local maximum in occupancy of binding site(s) Lrp-A to occur near [Lrp] = 5.5 nM, the physiologic concentration of free Lrp in the cell at 37° C.
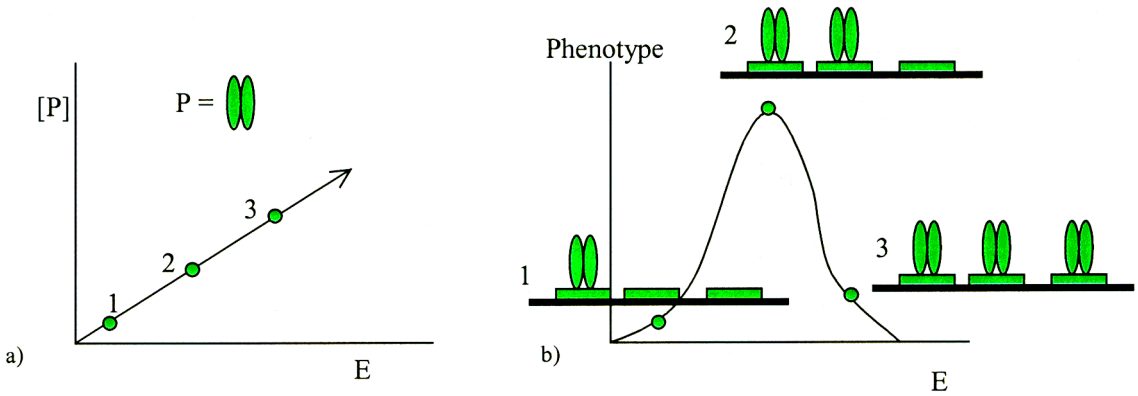
FIG. 9. Illustration of general mechanism for tuning phenotype to an environmental variable. (**a**) An environmental variable E monotonically controls the intracellular concentration and/or activity of a protein P. (**b**) Protein P binds to chromosomal DNA, and contributes to the regulation of a genetic process with phenotypic consequences. The chromosomal DNA has not just one binding site for P, but a number of them with varying binding affinities. When P occupies only the strong binding site, the genotype and associated phenotype is exaggerated, while when P occupies all the binding sites (strong plus weak), the genotype/phenotype is inhibited. Since P is controlled by an environmental variable E, and the occupancy of P's binding sites depends on the concentration of P, a local maximum (or minimum) in expression/phenotype is created as a function of the environmental variable E.
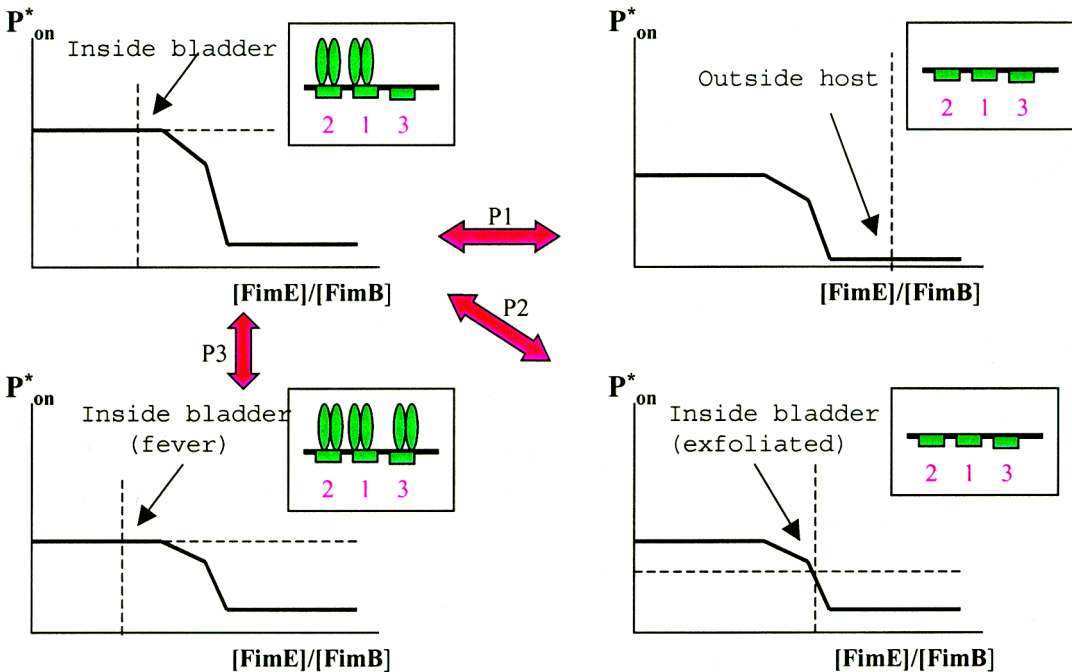
FIG. 10. *fim* network function in the infective process. Path P1: From outside the host to inside the bladder. A decrease in recombinase ratio and an increase in [Lrp] and Lrp-A occupancy transforms an unpiliated population into a piliated population. Pili allow *E. coli* to attach to and invade host cells. Path P2: Attachment to and invasion of host cells triggers exfoliation of the bladder epithelium. Exfoliated and lysed cells increase the medium richness, causing [Lrp] levels to fall and the recombinase ratio to rise. This shift increases response speed and detachment rate, and a decreases piliation level and attachment rate. Path P3: Attachment to and invasion of host cells triggers a fever in the host. The *fim* network senses the rise in temperature above 37°C through an increase in [Lrp] and Lrp-3 occupancy, and responds with a decrease in piliation level and attachment rate.

leucine complex binds nearly as well to Lrp-1 and Lrp-2 as does Lrp alone, but that Lrp-3 does not bind a Lrp-leucine complex. Thus, in the presence of leucine, more intracellular Lrp is required to bind Lrp-3 and initiate a decrease in switching frequency from its peak value. Since Lrp concentration increases with temperature, this switching maximum occurs at a higher temperature. Our model reproduces this effect.

INTEGRATION AND APPLICATION OF MODEL RESULTS

We now integrate the above analyses into a view of how the *fim* network is able to sense the environment and adaptively control phase variation behavior. We then apply this view to reconstruct *fim* network function in the course of a urinary tract infection, and to explain some experimental data.

fim *network response to environmental variables*

E. coli responds to its environment primarily by modulating the concentrations or activities of global regulatory proteins. These proteins in turn control genetic reaction circuits enabling the bacterium to adapt to its environment. Two of these global regulators, Lrp and H-NS, serve as inputs into the *fim* network. The *fim* regulatory circuit is designed to decode H-NS, Lrp, and amino acid concentrations into phase variation behavior, yielding piliation levels, response times, and host cell attachment, invasion and detachment rates suitable for life within or outside of a host. This control is accomplished in large part by two mechanisms: recombinase ratio control and a phenotype tuning motif.

Recombinase ratio control determines whether a population is strongly off, weakly on, or in transition. This motif translates H-NS levels, responsive to temperature and medium, into a recombinase ratio, which then serves as an input into a sigmoidal, switch-like piliation control function (Fig. 3). This control function is implemented by (a) differential repression by H-NS of the two recombinases, (b) competitive binding of the two recombinases to the invertible element, and (c) FimE's strong on-to-off switching bias in conjunction with a relatively unbiased FimB.

The other major environmental signals decoded by the *fim* circuit, intracellular Lrp and leucine concentrations, are transduced by a common environmental tuning motif (Figs. 8 and 9). At low levels, Lrp activates switching and increases piliation, while at high levels Lrp represses switching and decreases piliation, an effect amplified by leucine. This motif is implemented by two groups of energetically disparate binding sites (high affinity Lrp-A and low affinity Lrp-3) associated with different levels of phenotypic enhancement (higher and lower switching rates and piliation levels, respectively), and results in a circuit that is tuned to mammalian body temperature.

Recombinase ratio based control and the phenotype tuning motif intersect through the heights of the piliation control sigmoid asymptotes shown in Figure 3 (Table 2). The recombinase ratio determines whether the system is operating in the strongly off, weakly on, or transition regions. The Lrp binding site occupancy—by influencing switching rates and their ratios—determines how piliated an "on" population is and how fast the system responds to environmental changes. Together, these mechanisms create a piliation response surface that is sigmoidal along the [FimE]/[FimB] axis and (inverted) parabolic along the [Lrp] axis (Fig. 4).

The orientational control of *fimE* complements these controls. It increases the sensitivity of the *fim* network to the environment by making the circuit sensitive to [FimB] as well as to the recombinase ratio, and acts as source of memory for the switch, keeping it on long enough to construct pili. OC also reinforces the switching bias of *fimE* and prevents chatter, rapid indecisive switching between on and off states.

Together, these features allow the circuit to read the temperature and medium and actuate phase variation behaviors suitable for infection. How does the circuit function in the infection process? Since *fim* uses H-NS, Lrp, and amino acid levels to sense the environment, reconstruction of network operation through the infection process requires knowledge of the relationship between environmental conditions and recombinase and global regulator concentrations. Unfortunately, such a quantitative map has yet to be determined. It is known, however, that [Lrp], [FimB], and [FimE] increase with temperature and are inversely related to medium richness (Donato et al., 1997; Landgraf et al., 1996; Olsen and Klemm, 1994; Olsen et al., 1998; Oshima et al., 1995), and that, because of differential repression of *fimE* and *fimB* by H-NS, the recombinase ratio [FimE]/[FimB] is likely to be small at high temperatures and in poor media, as found in the blad-

der, and large at low temperatures or in rich media. This information, along with the results of our analysis, suggests a number of paths that might be traversed in the course of a urinary tract infection.

Pathways to infection

Temperature-based path from outside to inside of host and vice versa. Bacteria can use temperature to distinguish between a host environment (37°C) and the outside world (lower temperatures). The *fim* circuit creates piliated populations inside a host urinary tract, and unpiliated populations in the soil. Thus, infection transforms a strongly off population into a weakly on population. This transformation is accomplished through a decrease in recombinase ratio [FimE]/[FimB] and an increase in [Lrp] from a very low level (binding sites Lrp-A, Lrp-3 unoccupied) to an intermediate level (Lrp-A occupied, Lrp-3 unoccupied). The shift in recombinase ratio results in a right-to-left slide across the piliation sigmoids, while the change in Lrp binding site occupancies results in an increase of the maximal asymptote of these sigmoids. This trajectory is illustrated by P1 in Figure 10. Since the host cell attachment rate is proportional to piliation level, an increase in urothelial wall attachment results.

Temperature-based path within host, ascension process, and immune-triggered fever. There are two sources of temperature variation within an infection cycle. The first is the ascension process, where bacteria move from the gut to the perineum to the urinary tract. A second source of temperature variation within the host is from fever, which raises the temperature above 37°C in response to an infection. As shown in path P3 in Figure 10, this increase in temperature decreases piliation level and attachment rate, an adaptive response to the immune system activation signaled by the presence of fever. The environmental tuning motif of the *fim* network senses the rise in temperature through an increase in Lrp level and Lrp-3 occupancy, and responds by decreasing the maximal asymptotes of the control sigmoid (Fig. 10).

Medium-based path within host. A poor nutritional environment at 37°C can be found in the bladder, either before an immune response has been generated or in areas not under local immune attack. These conditions likely correspond to the maximum of the phenotype tuning motif (Lrp-A occupied, Lrp-3 unoccupied) and to a low value of [FimE]/[FimB], and thus the leftmost, high asymptotes of the switching functions P_{on} and τ (Fig. 3). Under these conditions the model predicts high piliation and attachment/invasion rates, and relatively slow off switching and detachment rates. When invasion leads to lysed or exfoliated host cells, the local environment becomes nutritionally richer, and more dangerous for bacteria because of the increased likelihood of being attacked by neutrophils or other phagocytes. Our model predicts that bacteria sense this threat through the increase in recombinase ratio and decrease in [Lrp] brought about by the change of medium, as illustrated in path P2 of Figure 10. The bacteria respond by lowering their piliation level and attachment rate and increasing their detachment rate.

Resolution of apparent inconsistencies in experimental data

Though the majority of experimental observations in Gally et al. (1993) and Roesch and Blomfield (1998) fall into self-consistent trends, some appeared to be inconsistent and were interpreted to mean that important pieces in the regulation of the *fim* switch had yet to be uncovered.

The data in question can be found in Roesch and Blomfield (1998) and Gally et al. (1993). Our model explains (1) why the FimB promoted switching rates differ in defined rich and min+IVLA media (Gally et al., 1993), (2) why in a Lrp-3⁻ mutant, the FimE promoted switching rate is smaller in minimal medium than in min+IVLA medium, though the FimB promoted switching rates are near-equal in the two media (Roesch and Blomfield, 1998), and (3) why the difference in FimB promoted switching in rich and minimal medium evident at lower temperatures all but disappears at 42°C, though differences in FimE promoted switching are still significant at this temperature (Gally et al., 1993).

1. Differences in FimB promoted switching rates in defined rich and min+IVLA media can be explained by the Lrp mediated temperature tuning mechanism (Figs. 8 and 9). Intracellular [Lrp] is greater in

minimal medium than in rich medium (Landgraf et al., 1996; Roesch and Blomfield, 1998). If the effect of greater intracellular [Lrp] in minimal medium on Lrp-A occupancy has a switch-rate enhancing effect that more than compensates for the accompanying decrease in amino acid levels, the model predicts a higher switching rate in poor than in rich medium, as observed (rich: 1.1×10^{-3}/cell/gen; min: 2.4×10^{-3}/cell/gen). When amino acids I,V, L, and A are added to minimal medium, the model predicts an even greater occupancy of binding site Lrp-A, but not Lrp-3, and thus a higher switching rate than that found in either minimal medium alone or rich medium (8.9×10^{-3}/cell/gen observed). Our model is consistent with these data; moreover, our model does not require a "factor present in defined rich medium, but absent or reduced in minimal medium, (blocking the) ability of Lrp and I,V,L, and A to stimulate FimB promoted switching" as hypothesized in (Gally et al., 1993), though such a factor may well exist.

2. The Lrp-3$^-$ mutant data can be explained by the Lrp mediated tuning mechanism in conjunction with recombinase ratio control (Fig. 3). Since in a *fimE*$^-$ mutant the main consequence of adding amino acids to the medium is to block Lrp-3 occupancy, the model predicts that adding I, V, L, and A to the medium will have no effect on FimB mediated switching, as observed. However, so-called FimE promoted switching is really wild-type switching (*fimB* is present), and thus subject to recombinase ratio control. If adding amino acids IVLA to the medium results in an increase in recombinase ratio [FimE]/[FimB], the model predicts a left-to-right shift along the $\tau(\gamma)$ control sigmoid and an accompanying increase in switching speed. This shift, along with the Lrp binding site occupancy changes, renders consistent all experimental results in (Roesch and Blomfield, 1998) without calling for missing network components.

3. An explanation of (3) consistent with our model is that at 42°C, Lrp concentrations are high enough (extreme temperature induced H-NS de-repression of *lrp* [Oshima et al., 1995]) to saturate Lrp-A and Lrp-3, regardless of differences in growth medium that affect [Lrp] at lower temperatures. Further, though Lrp binding site occupancies might be identical in rich and minimal medium at high enough temperatures, differences in [FimE]/[FimB] (and an accompanying slide along the recombinase ratio control sigmoid) could still exist. The former can account for the converging FimB promoted switching rates seen at high temperatures, and the latter for switch-off rate differences observed in the wild-type strain at 42°C.

CONCLUSION

Our model of the *fim* control network answers the questions regarding network operation and design posed in the introduction, and accounts for the data in Gally et al. (1993) and Roesch and Blomfield (1998). Our analysis yields hypotheses on the purpose of the two recombinase design, the role of orientational control in network function, the source of FimE on-to-off specificity, and the mechanism responsible for tuning pili expression to mammalian body temperature. It also explains some apparent contradictions in the experimental data, which had been interpreted to mean that important pieces of regulatory machinery have yet to be uncovered (Gally, et al., 1993; Roesch and Blomfield, 1998).

In the course of our analysis we identified a number of regulatory motifs active in the *fim* network: the invertible DNA element switch, the ratio-controlled sigmoid (Fig. 3), the phenotype tuner (Fig. 9), and state feedback as memory (*fimE* orientational control). The functions of these individual motifs are integrated to accomplish the overall circuit behavior. Indeed, this circuit function and its motifs can be abstracted into a stochastic pulse generator (Fig. 11) expressed in largely digital logic form. However, though such Boolean circuit diagrams are often useful analogies to those trained to read them, they often mask a good deal of the physical and dynamical complexity of the circuit. In Figure11, the depicted delays are non-standard elements with complicated probability distributions derived from the underlying mesoscopic model. These distributions and their implications for circuit function could not be derived without first solving the lower-level model. At this stage, while we are just beginning to identify and characterize regulatory motifs within genetic regulatory networks, such models and analyses are still necessary. But as the collection of increasingly well-characterized genetic circuit regulatory modules grows, it will be possible to reduce arbitrarily large and complex genetic circuit diagrams to a number of interconnected 'devices', thus rendering accurate higher level analyses of system properties possible (Rao & Arkin, 2001).

APPENDIX A: MATHEMATICAL MODEL

The invertible element switch. The equation below models the phase variation behavior of the basic *fim* switch in a single *E. coli* bacterial cell as a function of the intracellular free concentrations of controlling recombinases FimE and FimB, global regulators IHF and Lrp, and environmental factors such as temperature and leucine concentration:

$$\frac{dP_{on}}{dt} = f(1 - P_{on}) - gP_{on} \tag{1}$$

with

$$f = \frac{\sum_{s \epsilon OFF} \alpha_s e^{-\Delta G_s/RT}[IHF]^{n(s)}[FimE]^{j(s)}[FimB]^{k(s)}[Lrp^*]^{m(s)}[Lrp]^{l(s)}}{1 + \sum_{s \epsilon OFF} e^{-\Delta G_s/RT}[IHF]^{n(s)}[FimE]^{j(s)}[FimB]^{k(s)}[Lrp^*]^{m(s)}[Lrp]^{l(s)}},$$

and

$$g = \frac{\sum_{s \epsilon ON} \alpha_s e^{-\Delta G_s/RT}[IHF]^{n(s)}[FimE]^{j(s)}[FimB]^{k(s)}[Lrp^*]^{m(s)}[Lrp]^{l(s)}}{1 + \sum_{s \epsilon ON} e^{-\Delta G_s/RT}[IHF]^{n(s)}[FimE]^{j(s)}[FimB]^{k(s)}[Lrp^*]^{m(s)}[Lrp]^{l(s)}}.$$

Equation 1 describes the evolution of P_{on}, the probability of the piliation switch being in the on position, with time. P_{on} depends on [FimE], [FimB], [Lrp], and [IHF], the concentrations of unbound FimE, FimB, Lrp and IHF regulatory protein molecules in the cell. It also depends on ΔG_i, the Gibbs free energies of molecular configurations s = 1:36 described in Table 1. Other parameters include the gas constant R = 1.99 cal/mol/K, the temperature T in Kelvin, and switching rates α_i described in Table 3. These switching rates come in units of /cell/minute, and encapsulate the likelihood per unit time of a switching event given the realization of a
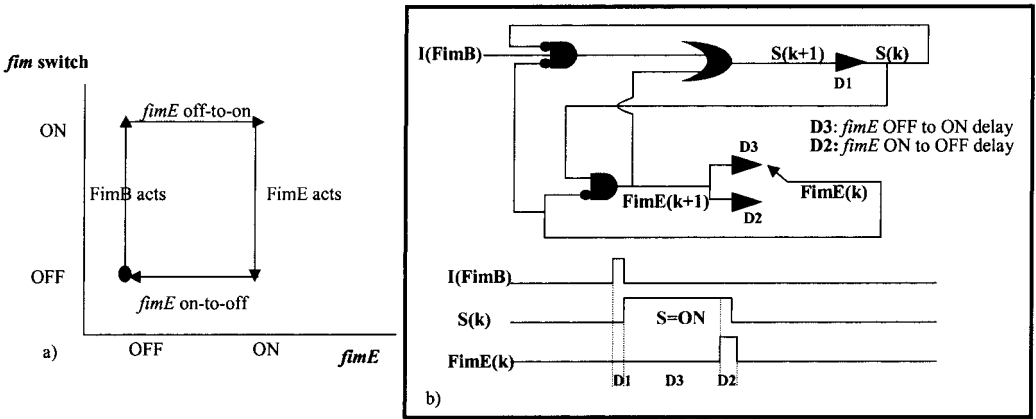
FIG. 11. The *fim* circuitry behaves like a pulse generator with stochastic delays. (**a**) The single stable state: the *fim* switch (*S*) is in the off position and *fimE* is not expressed. Upon reception of input signal FimB, the state switches from (*S* = OFF, *fimE* = OFF) to (*S* = ON, *fimE* = OFF). The switch stays on for a length of time (pulse width) governed by the log normal distribution shown in Figure 6, at which point the signal FimE turns the switch back off again and the system returns to its stable state. (**b**) Digital logic diagram of type 1 phase variation, where S is the switch state, I is the abstracted FimB mediated off-to-on signal, and FimE is the abstracted FimE mediated on-to-off signal.

particular molecular configuration. Configuration sets ON = {1–8; 17–26}, OFF = {9–16; 27–36}, and indices n(s), j(s), k(s), l(s) and m(s) represent the number of IHF, FimB, FimE, Lrp, and Lrp* (either Lrp or Lrp-leucine) molecules bound to the switch DNA in each of the 36 configurations of Table 1.

TABLE 1. STATE TABLE FOR THE *fim* SWITCH

State	P_{IHF}	$P_{FimE/B}$	Lrp-A	Lrp-3	ΔG	α	n	j	k	m	l
1/9	—	—	—	—	0	0	0	0	0	0	0
2/10	IHF	—	—	—	ΔG_2	0	1	0	0	0	0
3/11	IHF	FimE	—	—	$\Delta G_3/\Delta G_7$	α_1/α_4	1	0	1	0	0
4/12	IHF	FimB	—	—	$\Delta G_4/\Delta G_8$	α_2/α_3	1	1	0	0	0
5/13	IHF	FimE	Lrp*	—	$\Delta G_{31a}/\Delta G_{71a}$	$\alpha_{11a}/\alpha_{41a}$	1	0	1	2	0
6/14	IHF	FimE	Lrp*	Lrp	$\Delta G_{31b}/\Delta G_{71b}$	$\alpha_{11b}/\alpha_{41b}$	1	0	1	2	1
7/15	IHF	FimB	Lrp*	—	$\Delta G_{41a}/\Delta G_{81a}$	$\alpha_{21a}/\alpha_{31a}$	1	1	0	2	0
8/16	IHF	FimB	Lrp*	Lrp	$\Delta G_{41b}/\Delta G_{81b}$	$\alpha_{21b}/\alpha_{31b}$	1	1	0	2	1
17/27	—	FimE	—	—	$\Delta G_{33}/\Delta G_{77}$	0	0	0	1	0	0
18/28	—	FimB	—	—	$\Delta G_{44}/\Delta G_{88}$	0	0	1	0	0	0
19/29	—	FimE	Lrp*	—	$\Delta G_{331a}/\Delta G_{771a}$	0	0	0	1	2	0
20/30	—	FimE	Lrp*	Lrp	$\Delta G_{331b}/\Delta G_{771b}$	0	0	0	1	2	1
21/31	—	FimB	Lrp*	—	$\Delta G_{441a}/\Delta G_{881a}$	0	0	1	0	2	0
22/32	—	FimB	Lrp*	Lrp	$\Delta G_{441b}/\Delta G_{881b}$	0	0	1	0	2	1
23/33	—	—	Lrp*	—	$\Delta G_{3a}/\Delta G_{7a}$	0	0	0	0	2	0
24/34	—	—	Lrp*	Lrp	$\Delta G_{33a}/\Delta G_{77a}$	0	0	0	0	2	1
25/35	IHF	—	Lrp*	—	$\Delta G_{33b}/\Delta G_{77b}$	0	1	0	0	2	0
26/36	IHF	—	Lrp*	Lrp	$\Delta G_{31a}/\Delta G_{71a}$	0	1	0	0	2	1

This table lists the 36 molecular configurations allowed by our mathematical model, with states 1–8 and 17–26 corresponding to the switch in on position, and states 9–16 and 27–36 to the off position. The binding sites included in the switch model are (1) the IHF site P_{IHF}, an abstraction of the two IHF binding sites shown in Figure 1, (2) the FimE/FimB site $P_{FimE/B}$, an abstraction of the four FimE/FimB half-sites shown in Figure 1, (3) Lrp-A, an abstraction of cooperative Lrp binding sites 2 and 1, capable of binding two Lrp or Lrp-leucine complex dimers, and (4) the Lrp-3 site, Lrp binding site 3 in Figure 1 capable of binding a Lrp dimer, but not a Lrp-leucine complex. ΔG is the free energy of binding of a particular molecular configuration, and α is a switching rate associated with that configuration. Whenever two parameters x and y appear in this table as x/y, interpret x as the parameter value when the switch is in the on position, and y as the parameter value when the switch is in the off position. Where Lrp* appears in the table, one can substitute either Lrp or an Lrp-leucine complex, as they are thought to have nearly identical binding strengths when bound to Lrp-A. Indices n, j, k, l, and m denote the number of IHF, FimB, FimE, Lrp, and Lrp* (either Lrp or Lrp-leucine) molecules bound to the switch DNA in each configurational state.

To derive Equation 1 according to the assumptions and abstractions described in the Mathematical model assumptions section, we (a) wrote out a master equation describing the evolution of $P_{on}(t)$, $dP_{on}/dt = f(1 - P_{on}) - gP_{on}$ (Kampen, 1992), where f and g are transition probability rates, (b) created state Table 1 to codify our abstraction of what is known experimentally about the proteins that bind to/around the *fim* switch DNA, and how their binding contributes to the likelihood and speed of switching from on to off and from off to on, (c) applied the tenets of equilibrium statistical thermodynamics (Hill, 1960), as applied in Shea and Ackers (1985) and Wolf and Eeckman (1998) to derive expressions for the probabilities of the switch DNA being in any of the 18 possible configurations for each switch position, e.g., $p(3) = e^{-\Delta G3/RT}[IHF][FimE]/(1 + e^{-\Delta G2/RT}[IHF] + e^{-\Delta G3/RT} [IHF][FimE] + e^{-\Delta G4/RT}[IHF][FimB] + e^{-\Delta G31a/RT} [IHF][FimE][Lrp*]^2 + e^{-\Delta G31b/RT} [IHF][FimE][Lrp*]^2[Lrp] + e^{-\Delta G41a/RT}[IHF][FimB][Lrp*]^2 + e^{-\Delta G41b/RT} [IHF][FimB][Lrp*]^2[Lrp] + \ldots)$, (d) multiplied the probabilities of being in those molecular configurations allowing for switching (IHF and either FimE or FimB bound) by associated switching rates α_i, and (e) constructed f and g by summing the rate-scaled probability expressions to get $g = \alpha_1 p(3) + \alpha_2 p(4) + \alpha_{1la} p(5) + \alpha_{1lb} p(6) + \alpha_{2la} p(7) + \alpha_{2lb} p(8)$ and $f = \alpha_4 p(11) + \alpha_3 p(12) + \alpha_{4la} p(13) + \alpha_{4lb} p(14) + \alpha_{3la} p(15) + \alpha_{3lb} p(16)$.

The complete phase variation network model. We use a four state Markov model to represent the complete *fim* network in Figure 1, including *fimE* orientational control. A typical trajectory takes the system

from $P_{0,0}$ (S = OFF, *fimE* = OFF) to $P_{1,0}$ (S = ON, *fimE* = OFF) to $P_{1,1}$ (S = ON, *fimE* = ON) to $P_{0,1}$ (S = OFF, *fimE* = ON), and then back to $P_{0,0}$. Though more elaborate models are possible, this model explains the effect OC feedback has on the genetic network and is described by Equation 2:

$$
\frac{d}{dt}\begin{bmatrix} p_{1,1} \\ p_{0,1} \\ p_{0,0} \\ p_{1,0} \end{bmatrix} = \begin{bmatrix} -g(+) & f(+) & 0 & e_n \\ g(+) & -f(+)-e_f & 0 & 0 \\ 0 & e_f & -f(-) & g(-) \\ 0 & 0 & f(-) & -g(-)-e_n \end{bmatrix}\begin{bmatrix} P_{1,1} \\ P_{0,1} \\ P_{0,0} \\ P_{1,0} \end{bmatrix}
\tag{2}
$$

where $g(+)$ and $f(+)$ are the transition probability rates from Equation 1 with *fimE* = ON ([FimE] = [FimE]$_{ON}$), $f(-)$ and $g(-)$ are the transition probabilities from Equation 1 with *fimE* = OFF ([FimE] = [FimE]$_{OFF}$), e_f is rate at which *fimE* turns off once the switch turns off (orientational control), and e_n is the rate at which *fimE* turns on once the switch is turned back on again.

The bacterial population model. Because experiments in Gally et al. (1993) and Roesch and Blomfield (1998) track bacterial populations rather than individual cells, our model must provide information on how the percentage of switch-on bacteria is likely to change with time. If the reproduction rates of piliated and unpiliated bacteria are roughly the same (they are within 7% in stirred broth medium during exponential growth phase [Gally et al., 1993]), at each time t we expect the population to follow a Gaussian distribution with mean number of switch-on bacteria $\mu = NP_{on}(t)$ and variance $\sigma^2 = NP_{on}(t)(1 - P_{on}(t))$, where $P_{on}(t)$ is a solution of Equation 1 or 2 for a single bacterium and N is the size of the population. We employ this Gaussian assumption throughout the paper, allowing for the direct translation of single-cell model results to a population.

APPENDIX B: EXPRESSIONS FOR STEADY STATE PILIATION LEVEL, RESPONSE TIME, AND SWITCH-OFF DISTRIBUTION

We derived expressions for the following functions that together summarize phase variation behavior:

- P^*_{on}: The mean fraction of an *E. coli* population with switches in the on position—and thus presumably piliated—at steady state (during exponential growth phase).
- τ: A measure of the response speed of the switch, specifically the amount of time it takes $P_{on}(t)$ to reach 63.2% (1/e) of its steady state value P^*_{on} starting from an initial condition of $P_{on}(0) = 0$.
- $p_{on-off}(t')$: The on-to-off switching time probability distribution. The probability that the switch will turn off at time t = t' given that it was turned on at time t = 0.

In disease process terms, the significance of these functions is as follows: the rate at which bacteria attach to the urothelium is proportional to P^*_{on} ; the time it takes a bacterium to detach from a host cell is proportional to t', the length of time the switch is in the on position (with distribution $p_{on-off}[t']$); τ is a measure of the amount of time it takes a population to move from one steady state %ON to another in the event of a change in the environment (e.g., fever induced by immune response).

We analyzed the systems defined by Equations 1 and 2 for their steady-state behaviors using classical nonlinear analysis and bifurcation techniques (Guckenheimer and Holmes, 1997). The single stable stationary state $P^*_{on} = f/(f + g)$ and time constant $\tau = 1/(f + g)$ of Equation 1 completely characterize the behavior of the basic switch model (effect of recombinases and global regulators on the switch).

With *fimE* orientational control in operation, the single stable stationary state of the complete phase variation circuit in Figure 1, obtained by setting Equation 2 to zero and solving for $P^*_{on} = P^*_{1,1}+P^*_{1,0}$, is as follows:

$$
P^*_{on} = \frac{\dfrac{g(+)f(-)}{e_n} + \dfrac{f(+)f(-)}{e_f} + f(-)}{\dfrac{g(+)f(-)}{e_n} + \dfrac{f(+)f(-)}{e_f} + \dfrac{g(+)f(-)}{e_f} + \dfrac{g(+)g(-)}{e_n} + f(-) + g(+)}.
\tag{3}
$$

Expressions for the on-to-off probability distributions without and with *fimE* orientational control in effect are given, respectively, by the two equations below.

$$P(t')_{on \to off} = g \times e^{-gt'} \text{ without } fimE \text{ OC},\tag{4}$$

$$P(t')_{on \to off} = g(-)e^{-(g(-)+e_n)t'} + g(+)e^{-g(+)t'}(1 - e^{-e_n t'}) \text{ with } fimE \text{ OC}.\tag{5}$$

Figure 3, Figure 8, and Table 2 summarize how P^*_{on}, τ, and $p_{on\text{-}off}(t')$ depend on the recombinase and global regulator concentrations and physical parameters.

TABLE 2.   RECOMBINASE RATIO CONTROL PARAMETERS

Sigmoid parameter	*Dependencies*
$P^*_{on}(max)$	If $P_{FimE/B} = $ sat, $P^*_{on}(max)$ is a function of the ratio of FimB's on-to-off and off-to-on switching rates α_{2i}/α_{3i}, modulated by $r1_i$, the difference in cooperativity between FimB and IHF in the two switch positions, e.g., $1/(1 + (\alpha_2/\alpha_3)r1)$, with $$r1 = \frac{1 + e^{-(\Delta G88 - \Delta G8)/(RT)}/[\text{IHF}]}{1 + e^{-(\Delta G44 - \Delta G4)/(RT)}/[\text{IHF}]}.$$ If $P_{FimE/B} = $ u, $P^*_{on}(max)$ is a function of α_{2i}/α_{3i} modulated by $\Delta G_{4i} - \Delta G_{8i}$, the difference between binding affinities of FimB in the two switch positions, e.g., $1/(1 + (\alpha_2/\alpha_3)\exp(-(\Delta G_4 - \Delta G_8)/(RT)))$.
$P^*_{on}(min)$	If $P_{FimE/B} = $ sat, $P^*_{on}(min)$ is a function of the ratio FimE's on-to-off and off-to-on switching rates α_{1i}/α_{4i}, modulated by $r2_i$, the difference in cooperativity between FimE and IHF in the two switch positions, e.g., $1/(1 + (\alpha_1/\alpha_4)r2)$, with $$r2 = \frac{1 + e^{-(\Delta G77 - \Delta G7)/(RT)}/[\text{IHF}]}{1 + e^{-(\Delta G33 - \Delta G3)/(RT)}/[\text{IHF}]}.$$ If $P_{FimE/B} = $ u, $P^*_{on}(min)$ is a function of α_{1i}/α_{4i}, modulated by $\Delta G_{3i} - \Delta G_{7i}$, the difference between binding affinities of FimE in the two switch positions, e.g., $1/(1 + (\alpha_1/\alpha_4)\exp(-(\Delta G_3 - \Delta G_7)/(RT)))$.
$s1$	$s1$ is a function of $\Delta G_{4i} - \Delta G_{3i}$. It is steepest when FimB's S = ON binding affinity $(\Delta G_{4i}) >$ FimE's S = ON binding affinity (ΔG_{3i}).
$s2$	$S2$ is a function of $\Delta G_{7i} - \Delta G_{8i}$. It is steepest when FimE's S = OFF binding affinity $(\Delta G_{7i}) >$ FimB's S = OFF binding affinity (ΔG_{8i}).
$\tau(max)$	If $P_{FimE/B} = $ sat, $\tau(max)$ is a function of FimB's on-to-off and off-to-on switching rates, and the amount of cooperativity between FimB and IHF in the two switch positions, e.g., $$1\Big/\left(\frac{\alpha_2}{1 + e^{-(\Delta G44 - \Delta G4)/(RT)}/[\text{IHF}]} + \frac{\alpha_3}{1 + e^{-(\Delta G88 - \Delta G8)/(RT)}/[\text{IHF}]}\right).$$
$\tau(min)$	If $P_{FimE/B} = $ sat, $\tau(min)$ is a function FimE's on-to-off and off-to-on switching rates, and the amount of cooperativity between FimE and IHF in the two switch positions, e.g., $$1\Big/\left(\frac{\alpha_1}{1 + e^{-(\Delta G33 - \Delta G3)/(RT)}/[\text{IHF}]} + \frac{\alpha_4}{1 + e^{-(\Delta G77 - \Delta G7)/(RT)}/[\text{IHF}]}\right).$$

This table shows how the asymptote heights and transition region slopes of the recombinase ratio control sigmoids in Figure 3 depend on the physical parameters of the *fim* network. Because Lrp and recombinase binding site occupancies determine exactly which physical parameters dominate the heights and slopes of the control sigmoids (but not their functional forms), the parameter dependencies in the table are functions of a variable index, 'i' (e.g., α_{2i}/α_{3i}, where i = { }, la, or lb). For example, if [Lrp] is large enough to saturate binding sites Lrp-A and Lrp-A,3, the switching rate ratio dominating $P^*_{on}(max)$ is $\alpha_{2lb}/\alpha_{3lb}$, and the binding affinity difference dominating slope s1 is $\Delta G_{412} - \Delta G_{312}$. The example expressions in the table, meant to provide a flavor for the functional forms, are for the special case [Lrp] = 0 and no orientational control. The expression '$P_{FimE/B} = $ sat' in the table refers to the condition of significant intracellular recombinase concentration, leading to saturation or near saturation occupancy of switch binding site $P_{FimE/B}$. The expression '$P_{FimE/B} = $ u' in the table refers to the condition of very low intracellular recombinase concentrations, corresponding to minimal occupancy of site $P_{FimE/B}$. Expressions 'S = ON' and 'S = OFF' refer to on-and-off switch positions.

APPENDIX C: PARAMETER VALUES

Gally et al. (1993) fit a variety of experimental data to the following discrete linear model,

$$P_{on}(n + 1) = (1 - (k_1 + k_2 + k_3))P_{on}(n) + k_1, \tag{6}$$

where P_{on} is the percentage of an *E. coli* population with their switches on, n is the number of generations, and k_1, k_2 and k_3 are the FimB promoted off-to-on, FimB promoted on-to-off and FimE promoted on-to-off/cell/generation rates, respectively. To determine approximate switching efficiencies α_i for our model, we first discretized $dP_{on}/dt = f(1 - P_{on}) - gP_{on}$, to get the difference equation,

$$P_{on}(n + 1) = e^{-(f+g)t_{gen}}P_{on}(n) + (f/(f + g))(1 - e^{-(f+g)t_{gen}}), \tag{7}$$

where $t_{gen} \approx 20$ minutes, the time it takes a typical *E. coli* bacterial cell in exponential phase, in broth, to divide. Expanding the exponentials and equating first order terms in t_{gen} from Equations 6 and 7 leads to the assignments $k_1 = ft_{gen}$ and $k_2 + k_3 = gt_{gen}$. Further expansion of f and g results in the assignments $k_1 = \alpha_{3i}p(s_{3i})t_{gen}$ and $k'_3 = k_2 + k_3 = (\alpha_{2i}p(s_{2i}) + \alpha_{1i}p(s_{1i}))t_{gen}$ and ultimately in assignments $k_2 = \alpha_{2i}p(s_{2i})t_{gen}$ and $k_3 = \alpha_{1i}p(s_{1i})t_{gen}$. The parameters listed under k_3 in Gally et al. (1993) we call k'_3, because the measurements were taken on a *fimB$^+$ fimE$^+$* strain, not a *fimB$^-$* strain as necessary for a pure k_3 measurement. $k'_3 = k_2 + k_3$, the sum of switch-off rates due to FimB and FimE.

Other data used to calculate the switching rates α_{ji} are %ON at steady state $P^*_{on} \approx (\alpha_{3i} + \alpha_{4i})/(\alpha_{3i} + \alpha_{4i} + \alpha_{1i} + \alpha_{2i})$. Difficulties in estimating α_{ji} include (1) uncertainty about the probabilities of the system being in a particular molecular configuration during the experiment in which the data are collected, and (2) lack of a map from environmental conditions of nutrition and temperature to the concentrations of the recombinases and global regulators, and thus to the dominating parameters α_{ji} corresponding to each experimental condition.

TABLE 3. ESTIMATED SWITCHING RATES

Parameter	Estimated value	Switching rate
α_1	3.92×10^{-5}	FimE mediated On-to-Off
α_2	9.35×10^{-6}	FimB mediated On-to-Off
α_3	4.86×10^{-6}	FimB mediated Off-to-On
α_4	5.14×10^{-6}	FimE mediated Off-to-On
α_{11a}	0.006	FimE mediated On-to-Off, w/Lrp bound to Lrp-A
α_{21a}	6.8×10^{-4}	FimB mediated On-to-Off, w/Lrp bound to Lrp-A
α_{31a}	8.4×10^{-4}	FimB mediated On-to-Off, w/Lrp bound to Lrp-A
α_{41a}	2.57×10^{-4}	FimE mediated Off-to-On, w/Lrp bound to Lrp-A
α_{11b}	0.0006	FimE mediated On-to-Off, w/Lrp bound to Lrp-A and Lrp-3
α_{21b}	3.40×10^{-5}	FimB mediated On-to-Off, w/Lrp bound to Lrp-A and Lrp-3
α_{31b}	4.20×10^{-5}	FimB mediated Off-to-On, w/Lrp bound to Lrp-A and Lrp-3
α_{41b}	2.75×10^{-6}	FimE mediated Off-to-On, w/Lrp bound to Lrp-A and Lrp-3

These switching rate estimates were obtained using data from Gally et al. (1993) and Roesch and Blomfield (1998) as described in Appendix C.

To estimate α_1, α_2, α_3, and α_4, switching rates with [Lrp] = 0, we used the *lrp$^-$ fimB$^+$ fimE$^+$* and *lrp$^-$ fimB$^+$ fimE$^-$* switching and %ON data in Gally et al. (1993) and then solved the above simultaneous equations (with generation time $t_{gen} = 20$ min and configurational probability around $p = 0.5$). To estimate α_{11b}, α_{21b}, α_{31b}, and α_{41b}, the Lrp-A and Lrp-3 site saturation FimB- and FimE-mediated switching rates, we used the *fimE$^-$* and wild-type switching rate data at 42°C in Gally et al. (1993), along with the above equations. Our reasoning was that, according to data in Gally et al. (1993), *fimE$^-$* rates appear to converge at 42°C in poor and rich medium, suggesting that at 42°C [Lrp] has reached a saturation level in both types of media (if one believes that differing [Lrp] and [leucine] concentrations in rich and poor media at lower temperatures are responsible for the different switching rates observed). Also, if it is true that the local maximum seen in switching rates around 37°C correlates to a local maximum in Lrp-A (but not Lrp-3) occupancy,

and that higher temperatures imply higher Lrp concentrations (*lrp* repression by H-NS), then the Lrp-A and Lrp-3 sites should be closer to saturation at 42°C than at 37°C or 28°C. Clearly, experimental measurements of [Lrp] and Lrp binding site occupancies in different media at different temperatures, along with associated switching rates of various mutants, are necessary for better parameter estimates.

We estimated α_{11a}, α_{21a}, α_{31a} and α_{41a} by calculating the factors by which the FimB- and FimE-mediated switching rates were amplified as a result of knocking out Lrp-3 (Roesch and Blomfield, 1998), and then multiplied the switching data (processed as above) in Gally et al. (1993) by these factors. The data from Roesch and Blomfield (1998) could not be used directly because a different strain was used from that in Gally et al. (1993), with (at least in the *fimE⁻* case) quite different switching rates.

Table 4 lists some example binding affinities. As described in the caption, the binding affinities of Lrp and IHF to the switch DNA were calculated using experimental data from Murtin et al. (1998) and Roesch and Blomfield (1998), and the rest are typical values from Shea and Ackers (1985) and others. In our simulations, recombinase concentrations [FimB] and [FimE](on) were allowed to vary widely, though a range of 1–100 nM would be a reasonable guess. [FimE](off) was assumed less than [FimE](on)/100. Intracellular levels of free Lrp and leucine have been estimated at [Lrp] = 5.5 nM and [leucine] = 1.7–11.7 mM (Roesch and Blomfield, 1998).

TABLE 4.   SAMPLE ESTIMATED AND CALCULATED BINDING AFFINITIES

Parameter	Estimated value	Molecular configuration
ΔG_{ref}	-10^4	Reference binding energy (cal)
ΔG_2	$1.3 \times \Delta G_{ref}$	IHF bound, yielding 50% occupancy at .7 nM
ΔG_3	$\Delta G_2 + \beta_3 \times \Delta G_{ref}$	FimE, IHF bound, S = ON;
ΔG_4	$\Delta G_2 + \beta_4 \times \Delta G_{ref}$	FimB, IHF bound, S = ON
ΔG_7	$\Delta G_2 + \beta_7 \times \Delta G_{ref}$	FimE, IHF bound, S = OFF
ΔG_8	$\Delta G_2 + \beta_8 \times \Delta G_{ref}$	FimB, IHF bound, S = OFF
ΔG_{lrpA}	-24×10^3	Lrp dimers (2) bound to Lrp-A
$\Delta G_{lrpA,3}$	-36.3×10^3	Lrp dimers (3) bound to Lrp-A, Lrp-3
ΔG_{31a}	$\Delta G_3 + \beta_{31a} \times \Delta G_{lrpA}$	FimE, IHF, Lrp-A bound, S = ON
ΔG_{31b}	$\Delta G_3 + \beta_{31b} \times \Delta G_{lrpA,3}$	FimE, IHF, Lrp-A, Lrp-3 bound, S = ON
ΔG_{41a}	$\Delta G_4 + \beta_{41a} \times \Delta G_{lrpA}$	FimB, IHF, Lrp-A bound, S = ON
ΔG_{41b}	$\Delta G_4 + \beta_{41b} \times \Delta G_{lrpA,3}$	FimB, IHF, Lrp-A, Lrp-3 bound, S = ON
ΔG_{71a}	$\Delta G_7 + \beta_{71a} \times \Delta G_{lrpA}$	FimE, IHF, Lrp-A bound, S = OFF
ΔG_{71b}	$\Delta G_7 + \beta_{71b} \times \Delta G_{lrpA,3}$	FimE, IHF, Lrp-A, Lrp-3 bound, S = OFF
ΔG_{81a}	$\Delta G_8 + \beta_{81a} \times \Delta G_{lrpA}$	FimB, IHF, Lrp-A bound, S = OFF
ΔG_{81b}	$\Delta G_8 + \beta_{81b} \times \Delta G_{lrpA,3}$	FimB, IHF, Lrp-A, Lrp-3 bound, S = OFF

In our simulations, the terms $\beta_i \in (0.99, 1.01)$ were varied to experiment with different amounts of cooperativity, and the effect of different binding affinities. The binding affinities ΔG_2, ΔG_{lrpA}, and $\Delta G_{lrpA,3}$ were calculated, and the rest chosen as typical. Lrp-DNA binding affinities were calculated as follows. Data from Roesch and Blomfield (1998) specifies the concentration of Lrp (both alone and in the presence of leucine) required for half of the switch invertible element DNA to be bound by Lrp. Additionally, a shift mobility assay was used to show that at this concentration ([Lrp] = 2.4 nM, no leucine present), two stable Lrp-DNA species were present corresponding to Lrp being bound to sites Lrp-1,2 and −3 or exclusively to sites Lrp-1 and Lrp-2 (what we call Lrp-A). To figure out the missing free energy information, we added the two probability expressions in the caption below Figure 9, the sum of which is the probability that Lrp is bound to the switch DNA, set the sum to 0.5, and simplified to get $1.0 = \exp(-\Delta G_{Lrp-A}/RT)[Lrp]^2 + \exp(-\Delta G_{Lrp-A,3}/RT)[Lrp]^3$. Plugging in [Lrp] = 2.4 nM, and assuming near equal presence of the two Lrp-DNA species at this concentration, produces the estimate $(\Delta G_{Lrp-A}; \Delta G_{Lrp-A,3}) \approx (-24 \text{ kcal}; -36.3 \text{ kcal})$. Binding affinity ΔG_2 was determined in a similar fashion, using data from (Murtin et al., 1998) and estimating a 40–60% IHF binding site occupancy at a concentration of [IHF] = 0.7 nM. The ΔG's for molecular configurations 17–26 in Table 1 were estimated in an analogous fashion to those listed above.

REFERENCES

ABRAHAM, J.M., FREITAG, C.S., CLEMENTS, J.R., et al. (1985). An invertible element of DNA controls phase variation of type 1 fimbriae of *Escherichia coli*. Proc Natl Acad Sci USA **82,** 5724–5727.

ALON, U., SURETTE, M.G., BARKAI, N., et al. (1999). Robustness in bacterial chemotaxis. Nature **397,** 168–171.

BARKAI, N., and LEIBLER, S. (1997). Robustness in simple biochemical networks. Nature **387,** 913–917.

BARNETT, B.J., and STEPHENS, D.S. (1997). Urinary tract infection: an overview. Am J Med Sci **314,** 245–249.

BERGAN, T. (1997). *Urinary Tract Infections* (Basel: Karger).

BLOMFIELD, I.C., KULASEKARA, D.H., and EISENSTEIN, B.I. (1997). Integration host factor stimulates both FimB- and FimE-mediated site- specific DNA inversion that controls phase variation of type 1 fimbriae expression in *Escherichia coli*. Mol Microbiol **23,** 705–717.

BORST, D.W., BLUMENTHAL, R.M., and MATTHEWS, R.G. (1996). Use of an in vivo titration method to study a global regulator: effect of varying Lrp levels on expression of gltBDF in *Escherichia coli*. J Bacteriol **178,** 6904–6912.

BYKOWSKI, T., and SIRKO, A. (1998). Selected phenotypes of ihf mutants of *Escherichia coli*. Biochimie **80**(12), 987–1001.

CONNELL, I., AGACE, W., KLEMM, P., et al. (1996). Type 1 fimbrial expression enhances *Escherichia coli* virulence for the urinary tract. Proc Natl Acad Sci USA **93,** 9827–9832.

DONATO, G.M., LELIVELT, M.J., and KAWULA, T.H. (1997). Promoter-specific repression of fimB expression by the *Escherichia coli* nucleoid-associated protein H-NS. J Bacteriol **179,** 6618–6625.

FREE, A., and DORMAN, C.J. (1995). Coupling of *Escherichia coli* hns mRNA levels to DNA synthesis by autoregulation: implications for growth phase control. Mol Microbiol **18,** 101–113.

GALLY, D.L., BOGAN, J.A., EISENSTEIN, B.I., et al. (1993). Environmental regulation of the fim switch controlling type 1 fimbrial phase variation in *Escherichia coli* K-12: effects of temperature and media. J Bacteriol **175,** 6186–6193.

GALLY, D.L., LEATHART, J., and BLOMFIELD, I.C. (1996). Interaction of FimB and FimE with the fim switch that controls the phase variation of type 1 fimbriae in *Escherichia coli* K-12. Mol Microbiol **21,** 725–738.

GORDON, D.M., and RILEY, M.A. (1992). A theoretical and experimental analysis of bacterial growth in the bladder. Mol Microbiol **6,** 555–562.

GUCKENHEIMER, J., and HOLMES, P. (1997). *Nonlinear Oscillations, Dynamical Systems, and Bifurcations of Vector Fields*, 5th ed. (New York: Springer).

HILL, T.L. (1960). *An Introduction to Statistical Thermodynamics* (Reading, MA: Addison-Wesley).

HOOTON, T.M., and STAMM, W.E. (1997). Diagnosis and treatment of uncomplicated urinary tract infection. Infect Dis Clin North Am **11,** 551–581.

JONES, C.H., PINKNER, J.S., ROTH, R., et al. (1995). FimH adhesin of type 1 pili is assembled into a fibrillar tip structure in the *Enterobacteriaceae*. Proc Natl Acad Sci USA **92,** 2081–2085.

KAMPEN, N.G.V. (1992). *Stochastic Processes in Physics and Chemistry*, Rev. ed. (New York: North-Holland).

KLEMM, P. (1986). Two regulatory fim genes, fimB and fimE, control the phase variation of type 1 fimbriae in *Escherichia coli*. EMBO J **5,** 1389–1393.

KOMANO, T. (1999). Shufflons: multiple inversion systems and integrons. Annu Rev Genet **33,** 171–191.

KULASEKARA, H.D., and BLOMFIELD, I.C. (1999). The molecular basis for the specificity of fimE in the phase variation of type 1 fimbriae of *Escherichia coli* K-12. Mol Microbiol **31,** 1171–1181.

LAN, C.Y., and IGO, M.M. (1998). Differential expression of the OmpF and OmpC porin proteins in *Escherichia coli* K-12 depends upon the level of active OmpR. J Bacteriol **180,** 171–174.

LANDGRAF, J.R., WU, J., and CALVO, J.M. (1996). Effects of nutrition and growth rate on Lrp levels in *Escherichia coli*. J Bacteriol **178,** 6930–6936.

LANGERMANN, S., PALASZYNSKI, S., BARNHART, M., et al. (1997). Prevention of mucosal *Escherichia coli* infection by FimH-adhesin-based systemic vaccination. Science **276,** 607–611.

MARTINEZ, J.J., MULVEY, M.A., SCHILLING, J.D., et al. (2000). Type 1 pilus–mediated bacterial invasion of bladder epithelial cells. EMBO J **19,** 2803–2812.

MCADAMS, H.H., and ARKIN, A. (1997). Stochastic mechanisms in gene expression. Proc Natl Acad Sci USA **94,** 814–819.

McCLAIN, M.S., BLOMFIELD, I.C., and EISENSTEIN, B.I. (1991). Roles of fimB and fimE in site-specific DNA inversion associated with phase variation of type 1 fimbriae in *Escherichia coli*. J Bacteriol **173,** 5308–5314.

MULVEY, M.A., SCHILLING, J.D., MARTINEZ, J.J., et al. (2000). Bad bugs and beleaguered bladders: interplay between uropathogenic *Escherichia coli* and innate host defenses. Proc Natl Acad Sci USA **97,** 8829–8835.

MURTIN, C., ENGELHORN, M., GEISELMANN, J., et al. (1998). A quantitative UV laser footprinting analysis of the interaction of IHF with specific binding sites: re-evaluation of the effective concentration of IHF in the cell. J Mol Biol **284,** 949–961.

O'GARA, J.P., and DORMAN, C.J. (2000). Effects of local transcription and H-NS on inversion of the fim switch of *Escherichia coli*. Mol Microbiol **36,** 457–466.

OLSEN, P.B., and KLEMM, P. (1994). Localization of promoters in the fim gene cluster and the effect of H-NS on the transcription of fimB and fimE. FEMS Microbiol Lett **116,** 95–100.

OLSEN, P.B., SCHEMBRI, M.A., GALLY, D.L., et al. (1998). Differential temperature modulation by H-NS of the fimB and fimE recombinase genes which control the orientation of the type 1 fimbrial phase switch. FEMS Microbiol Lett **162,** 17–23.

OSHIMA, T., ITO, K., KABAYAMA, H., et al. (1995). Regulation of lrp gene expression by H-NS and Lrp proteins in *Escherichia coli*: dominant negative mutations in lrp. Mol Gen Genet **247,** 521–528.

PALLESEN, L., MADSEN, O., and KLEMM, P. (1989). Regulation of the phase switch controlling expression of type 1 fimbriae in *Escherichia coli*. Mol Microbiol **3,** 925–931.

RAO, C.V., and ARKIN, A.P. (2001). Control motifs for intracellular regulatory networks. Annu Rev Biomed Eng **3,** 391–419.

ROESCH, P.L., and BLOMFIELD, I.C. (1998). Leucine alters the interaction of the leucine-responsive regulatory protein (Lrp) with the fim switch to stimulate site-specific recombination in *Escherichia coli*. Mol Microbiol **27,** 751–761.

RUSSELL, P.W., and ORNDORFF, P.E. (1992). Lesions in two *Escherichia coli* type 1 pilus genes alter pilus number and length without affecting receptor binding. J Bacteriol **174,** 5923–5935.

RUSSO, F.D., and SILHAVY, T.J. (1991). EnvZ controls the concentration of phosphorylated OmpR to mediate osmoregulation of the porin genes. J Mol Biol **222,** 567–580.

SAUER, F.G., MULVEY, M.A., SCHILLING, J.D., et al. (2000). Bacterial pili: molecular mechanisms of pathogenesis. Curr Opin Microbiol **3,** 65–72.

SCHAEFFER, A.J., HULTGREN, S.J., and DUNCAN, J.L. (1987). Relationship of type 1 pilus expression in *Escherichia coli* to ascending urinary tract infections in mice. Infec Immun **2,** 373–380.

SCHILLING, J.D., MULVEY, M.A., VINCENT, C.D., et al. (2001). Bacterial invasion augments epithelial cytokine responses to *Escherichia coli* through a lipopolysaccharide-dependent mechanism. J Immunol **166,** 1148–1155.

SHEA, M.A., and ACKERS, G.K. (1985). The OR control system of bacteriophage lambda. A physical-chemical model for gene regulation. J Mol Biol **181,** 211–230.

STENTEBJERG-OLESEN, B., CHAKRABORTY, T., and KLEMM, P. (2000). FimE-catalyzed off-to-on inversion of the type 1 fimbrial phase switch and insertion sequence recruitment in an *Escherichia coli* K-12 fimB strain. FEMS Microbiol Lett **182,** 319–325.

TOMINAGA, A., IKEMIZU, S., and ENOMOTO, M. (1991). Site-specific recombinase genes in three *Shigella* subgroups and nucleotide sequences of a pinB gene and an invertible B segment from *Shigella boydii*. J Bacteriol **173,** 4079–4087.

UEGUCHI, C., KAKEDA, M., and MIZUNO, T. (1993). Autoregulatory expression of the *Escherichia coli* hns gene encoding a nucleoid protein: H-NS functions as a repressor of its own transcription. Mol Gen Genet **236,** 171–178.

VAN DE PUTTE, P., CRAMER, S., and GIPHART-GASSLER, M. (1980). Invertible DNA determines host specificity of bacteriophage mu. Nature **286,** 218–222.

WANG, Q., WU, J., FRIEDBERG, D., et al. (1994). Regulation of the *Escherichia coli* lrp gene. J Bacteriol **176,** 1831–1839.

WOLF, D.M., and EECKMAN, F.H. (1998). On the relationship between genomic regulatory element organization and gene regulatory dynamics. J Theor Biol **195,** 167–186.

Address reprint requests to:
Dr. Denise M. Wolf
Lawrence Berkeley National Laboratory
1 Cyclotron Road
Berkeley, CA 94720

E-mail: dmwolf@lbl.gov